



Norwegian University of  
Science and Technology

# Antenna system for a ground station communicating with the NTNU Test Satellite (NUTS)

**Beathe Hagen Stenhaug**

Master of Science in Electronics

Submission date: July 2011

Supervisor: Odd Gutteberg, IET



## Problem Description

NTNU is planning to develop and launch a student satellite named “NUTS”. This satellite will need a ground station for transmitting commands and receiving telemetry. The ground station will be located at NTNU premises, utilizing the existing antenna pedestal.

The task is to analyze, design, build and test a scale model antenna system for this ground station. The work should focus on an array antenna consisting of either 2 or 4 helical elements.

The preliminary specifications are

- Center frequency: 437 MHz.
- Bandwidth: The bandwidth should as a minimum, cover the actual amateur frequency band [435-439 MHz], as well as the anticipated Doppler shift.
- Antenna gain: Approximately 12 - 20 dB. The actual gain will be based on the revised link budget.
- Interface: Compatible with the receiver/transmitter to be used.
- Steerability: 0 - 360 degrees in azimuth and 0 - 180 degrees in elevation.
- Environmental specification: Operational wind velocity: 15 m/s.

In addition to designing and building the antenna system, a feasibility study of the various available tracking systems should be carried out.

Assignment given: February 2011

Supervisor: Odd Gutteberg, IET

## Preface

This document is my master thesis carried out in the spring of 2011 at the Department of Electronics and Telecommunication (IET) at the Norwegian University of Science and Technology (NTNU). NTNU is the third university to join the ANSAT (Norwegian Student Satellite Program), and the goal with ANSAT is to have three student satellites launched before the end of 2014. NTNU is in charge of one satellite, while the two others are controlled by students at University of Oslo (UiO) and Narvik University College (HiN). With the two earlier national student satellite projects NCUBE1 and NCUBE2 included, this satellite is going to be the 5th student satellite in Norway.

The student satellite project at NTNU is named NUTS after NTNU Test Satellite, and this thesis concentrates on the ground segment. In January 2011, NTNU was the only of the three universities that did not have its own ground station. During the spring of 2011 this has changed, and now the first signal from other student satellites has been received with our ground equipment. At the point of writing, the antennas at the ground station consists of two off-the-shelf Yagi Uda antennas, one for 145 MHz and one for 437 MHz. Both are frequencies for telemetry purpose. Later the Yagi Uda for 437 MHz will be replaced by an in-house designed and built helical antenna array.

This thesis is divided into two parts. The first part gives some general description of the ground station. The second part gives a more detailed description about helical antennas, including theory, design, simulation, construction and measurements.

To see the ground station slowly assemble has been a very interesting process, and designing a helical antenna has proved rewarding. To overcome problems in the design process and actually get to the stage where I could measure on a scale model in the anechoic chamber has been extremely interesting. I have been motivated for this work by the fact that the helical antenna may one day be used to communicate with the up-and-coming NUTS. For the future, I hope that another student will continue my work, build the antennas in real scale and mount them on the antenna rig on the roof.

## Acknowledgments

I would like to thank my supervisor Professor Odd Gutteberg for the support and all the productive inputs. I would also like to thank Project Manager Roger Birkeland and Institute Engineer Terje Mathisen for assisting me with the simulation program and at the antenna laboratory. A special thanks go to Irene Jensen at SINTEF for being a valuable source of information when it comes to antenna design. The Engineers at the mechanical workshop at the Institute deserves credit for making the antenna model with the ground conductors on short notice. Amanuensis in Geodesy Terje Skogseth has my gratitude for lending and teaching me how to use the theodolite. The other students at the NUTS project have my appreciation for the social aspect at the roof lab, especially Asbjørn Dahl for the constructive discussions about the radio system. At last I would also express my thankfulness to my friends Ida Onshus and Sindre Myren for proof-reading this thesis.

Trondheim, July 12th 2011

Beathe Hagen Stenhaus, LA3RTA

## **Abstract**

This thesis describes the design process of a helical antenna for the ground station at NTNU. The helical antenna is designed for the proposed telemetry link at 437 MHz. The main focus areas have been to be able to make the helical antenna small enough to be safely mounted on the roof of the building belonging to the Department of Electronics and Telecommunication, while at the same time having a big enough helical antenna to achieve the required gain, which is 16 dB. An earlier link budget has been revisited and the requirements has been adjusted accordingly. The theory section provides the equations that the design is based on. In the design and simulation section, articles from the Institute of Electrical and Electronics Engineers (IEEE) have been useful to see if the calculated design with wanted characteristics is achievable. The simulation process gives an understanding of what happens with the electromagnetic field and the gain when different physical dimensions are changed. A scale model has been constructed and measurements have been done in the anechoic chamber. The measurements shows an agreement with the simulations. The evaluation shows that it is sufficient with two antennas in an array, instead of four which has been previously proposed.

# Contents

<b>1</b>	<b>Background and introduction</b>	<b>1</b>
<b>I</b>	<b>Ground station</b>	<b>3</b>
<b>2</b>	<b>Link budget</b>	<b>4</b>
2.1	The revised link budgets . . . . .	4
2.2	Comments . . . . .	9
<b>3</b>	<b>Antenna system</b>	<b>10</b>
<b>4</b>	<b>Interface between the antenna and the ground station system</b>	<b>12</b>
4.1	Different tracking systems . . . . .	12
4.2	Tracking programs . . . . .	13
<b>5</b>	<b>Local environment</b>	<b>15</b>
5.1	Horizon outline . . . . .	15
5.2	Wind . . . . .	17
<b>II</b>	<b>Helical antenna</b>	<b>19</b>
<b>6</b>	<b>Theory</b>	<b>20</b>
6.1	Classic physical structure . . . . .	20
6.1.1	Electrical properties . . . . .	21
6.1.2	Mechanical properties . . . . .	22
6.1.3	Ground conductor . . . . .	22
6.2	Other possibilities for physical structure . . . . .	23
6.3	Characterization of antenna and antenna system . . . . .	24
6.3.1	Directivity . . . . .	24
6.3.2	Gain . . . . .	24
6.3.3	Antenna efficiency . . . . .	25
6.3.4	Polarization . . . . .	25
6.3.5	Radiation pattern . . . . .	27
6.3.6	Antenna array . . . . .	29

6.3.7	Input impedance . . . . .	30
6.3.8	Scattering parameters . . . . .	30
6.3.9	Voltage standing wave ratio . . . . .	30
6.3.10	Return loss . . . . .	31
<b>7</b>	<b>Antenna design and simulation</b>	<b>32</b>
7.1	Preliminary antenna design . . . . .	32
7.2	Simulation . . . . .	34
7.2.1	Parameter variation . . . . .	35
7.2.2	Final design . . . . .	37
7.2.3	Difficulties . . . . .	40
<b>8</b>	<b>Final design and construction</b>	<b>41</b>
8.1	Geometrical scaling . . . . .	41
8.2	Impedance matching . . . . .	43
<b>9</b>	<b>Measurements and results</b>	<b>45</b>
9.1	Instrumentation . . . . .	45
9.2	Measurement explanations . . . . .	46
9.3	Results . . . . .	47
9.3.1	Gain . . . . .	47
9.3.2	Impedance matching . . . . .	48
<b>10</b>	<b>Discussion</b>	<b>50</b>
<b>11</b>	<b>Conclusion</b>	<b>52</b>
11.1	Future work . . . . .	52
<b>III</b>	<b>Appendices</b>	<b>57</b>
<b>A</b>	<b>NUTS-1 Mission Statement</b>	<b>58</b>
<b>B</b>	<b>Simulation results</b>	<b>65</b>
<b>C</b>	<b>The helical antenna model with ground conductors</b>	<b>72</b>
<b>D</b>	<b>Measuring results</b>	<b>76</b>
D.1	Measurements with the flat ground conductor . . . . .	77
D.2	Measurements with the cupped ground conductor . . . . .	83
D.3	Measurements with the truncated cone ground conductor . . . . .	87
D.4	Comparison between measurements with the three different ground conductors . . . . .	91
D.5	Impedance matching . . . . .	92

## List of Abbreviations

ADS	Advanced Design System
AMSAT	Radio Amateur Satellite Corporation
ANSAT	Norwegian Student Satellite Program
ARK	Academic Radio Club
EIRP	Effective Isotropic Radiated Power
GMSK	Gaussian Minimum Shift Keying
HPBW	Half Power Beam Width
HiN	Narvik University College
IARU	International Amateur Radio Union
IEEE	Institute of Electrical and Electronics Engineers
IET	Department of Electronics and Telecommunication
LHC	Left-Handed Circular polarization
LNA	Low Noise Amplifier
NAROM	Norwegian Centre for Space-related Education
NTNU	Norwegian University of Science and Technology
NUTS	NTNU Test Satellite
PA	Power Amplifier
RHC	Right-Handed Circular polarization
SNR	Signal to Noise Ratio
TT&C	Telemetry, Tracking and Command
UHF	Ultra High Frequency
UiO	University of Oslo

# Chapter 1

## Background and introduction

Less than a year has passed since NTNU became part of the national student satellite program and a project manager was hired. Since then, much has happened with the student satellite project. More students have been involved and the project manager has made it more organized in addition to supervise each sub section. Ten students from different departments were involved in the spring of 2011, and they had regular meetings during the semester so each person was aware of the others, during the whole period.

In the communication section, the previously proposed<sup>1</sup> radio amateur band, (144-146 MHz and 435-439 MHz), is still going to be used for telemetry, tracking and command (TT&C). The satellite will have one transceiver for each frequency. Since the main payload is going to be an IR-camera for atmospheric observations, there is an additional need for a high speed link. This is a task for future project or master students. As an extra payload, a concept for a wireless short range data bus connecting different subsystems will be added.

The satellite system is not complete without a ground station that is able to communicate with the satellite. There are ground stations both in the local area and in other parts of Norway, which can transmit and receive on the frequencies that NUTS will use. However, to gain easier access to the satellite, NTNU will have its own ground station. During the spring of 2011 the ground station has changed from being a description on paper to become an actual structure, composed of antennas on a steerable rig connected to a radio indoor. The radio is linked to a computer that uses software to track and download signals from satellites that passes NTNU in their orbits. Several students and the project manager have taken the radio amateur license and can now legally operate the ground station.

This work is concentrated on the ground station antenna that will operate at 437 MHz, which are frequencies situated in the Ultra High Frequency (UHF) band, and it is based on the work of two earlier students at NTNU, Mireia Oliver Miranda[1] and Laurea Maigistrale[2]. However, an updated revision of

---

<sup>1</sup>Latest proposed in: Feasibility Study of a Ground Station for NTNU Test Satellite, 2011 by Beathe Hagen Stenhaus

the link budget shows that the specification for the ground station is not as strict as previously understood. This made it possible to make a physically smaller antenna design, which is the reason why the work of the earlier students is not directly continued. Additionally, a different simulation program has been used, namely CST MICROWAVE STUDIO instead of Agilent EMDS and WIPL-D.

As mentioned, this thesis is divided into two parts. The first part of this thesis deals with the ground station. In this first part there are four chapters. Chapter 2 presents the link budget and explains some of the most vital parameters in it. Chapter 3 includes a short overview of the system around the antenna, also understood as the complete ground station. Chapter 4 describes the interface between the antenna and the radio system including different tracking systems and programs. Chapter 5 concerns about the local environment and introduces a horizon outline and discusses some aspects dealing with wind load on an antenna structure.

The second part of thesis has six chapters, which treat the helical antenna. Chapter 6 presents the theory of helical antennas. Chapter 7 explains the design and simulation process, including simulation results. Chapter 8 describes the final design with the scaled model. Chapter 9 reveal the measurement results, where most of the plots are added in Appendix D. Chapter 10 discusses the results and finally Chapter 11 draws a conclusion and point out the remaining work for future students.

## Part I

# Ground station

## Chapter 2

# Link budget

### 2.1 The revised link budgets

The link budget states requirements and limitations of the antenna design. A more thorough explanation of the parameters in the link budget are presented in “Feasibility Study of a Ground Station for NTNU Test Satellite”[3], however, the explanation of the revised results is presented here in addition to definitions of the most important parameters.

To be certain that the signal sent from the satellite will be detectable with the equipment at ground level, proper margins must be implemented. The system’s overall performance is described by the parameters Signal to Noise Ratio (SNR) and energy per bit over noise spectral density,  $E_b/N_0$ .

Fading margin describes how much additional fading a system can have, without degrading the system performance. The fading margin should be big enough to ensure that the system has good performance most of the time, but at the same time it should not include rare atmospheric effects.

The downlink and uplink budgets, see Table 2.1 and Table 2.2, are made in cooperation with the student working on the radio system on the student satellite. The updates in the link budget are found in most of the changeable parameters, and a short description follows. The description is divided into the same subsections as in the link budget, for an easier comparison.

**Common parameters** The Baud rate is adjusted down to 9600 symbols per second for downlink, since this frequency has been decided to be telemetry back up link, and the larger bit rates will occur at other frequencies.

**Noise properties** The system noise temperature is approximately equal the sum of the antenna noise temperature and the LNA noise temperature[4]. The downlink budget concerns with the ground station antenna. The main sources of noise are sky noise and ground noise. The sky noise is gathered from the main lobe, which originates from the radiation from the sun and the moon, absorption,

re-emission by oxygen, etc. However, it is assumed that the antenna not will point directly at the sun. From figure 7.12 in [5], the brightness temperature of a clear sky is about 17 K for operating frequency of 1 GHz, when the curve is extrapolated and when seen with an elevation of 5 degrees. The brightness temperature used for 437 MHz is therefore 15 K. The ground noise is primarily picked up at the side and back lobes. The earth radiates at about 290 K, so it is not wanted for the antenna to receive too much of that noise. If the antenna in the main, side and back lobes together receive 2/3 of the sky and 1/3 of the ground<sup>1</sup>, then the antenna temperature would be about 110 K. The ground station has so far no LNA, but it is expected that it will be useful to add one later. SP 7000[6] is a low noise GaAsFET mast mounted preamplifier used at other ground stations, including the one in Oslo, for the frequency band 430/440 MHz. The SP 7000 has a noise factor of 0.9 dB, which gives a noise temperature of 70 K, according to the relation  $NF = 1 + T/T_0$ , where  $T_0$  is set to 290 K. In total, the system noise temperature at the ground station antenna will be approximately 180 K.

The uplink budget concerns about the satellite antenna, and the main sources of noise are the earth and outer space. The work on the antenna design at the satellite has not continued after 2007, but it is assumed that it will be some kind of dipole. Dipoles have omnidirectional radiation patterns shaped like a toroid. If half of the radiation pattern receives noise from the earth radiation ( $\sim 290K$ ) and the other half receives noise from outer space ( $\sim 3K$ ), then the antenna temperature will be about 150 K. On the other hand, the satellite will probably not see that much of the earth at the same time. Yet this conservative result is kept, at least until the radiation properties for the satellite antenna are decided. The low noise amplifier in the satellite is a SGL 0662Z[7]. For the frequency 450 MHz the LNA has a noise factor of 0.84, which gives a noise temperature of about 60 K. Then the total system noise temperature at the satellite will be approximately 210 K.

The noise bandwidth at downlink is set to 15 000 Hz, which is the bandwidth of the narrowest filter in the Icom IC-9100 radio. On uplink the noise bandwidth is set to 40 000 Hz, which is the filter bandwidth in the satellite, estimated from the bit rate, the expected Doppler shift and an additional temperature drift.

**Orbit parameters** The worst case for communication for the satellite is adjusted down from 20 to 5 degrees over the horizon. The worst case is taken from the measurements in Section 5.1. From the horizon outline it can be seen that there are 3 degrees between true and visible horizon most of the time. An elevation of 5 degrees was chosen as a worst case since that would include more of the time. The change in worst case elevation also changes the maximum distance and free space loss, so new values are calculated.

---

<sup>1</sup>These ratios are estimated after the radiation pattern for the helical antenna with cupped ground conductor, see Figure D.7 in Appendix D.

**The ground station and the satellite as a transmitter** The satellite as a transmitter, has new values for transmitted power and gain and the best case is now 1 W and 2 dB and the worst case is 0.3 W and 2 dB for power and gain respectively. These values were adjusted down from 1 W and 5.77 dB after a discussion with the student designing the radio transceiver in the satellite, except that the best case transmitted power is kept the same. The radio at the ground station can transmit maximum 75 W at the 430/440 MHz band[8], so 75 W will be the transmitted power if necessary. It should be kept in mind that this might be too much power under good conditions, such as when the satellite is in zenith, when the transmitted power in some cases must be adjusted down. In this way the satellite receives an appropriate amount of power. The gain at the ground station is adjusted down from 20 dB, which was found too much, to 16 dB, which suffice for this frequency.

The total transmission line loss in the satellite is preliminary set to be 2.2 dB, a value taken from a generic link budget model from Radio Amateur Satellite Corporation (AMSAT) and International Amateur Radio Union (IARU)[9]. The loss in the cables at the ground station is measured to be about 8 dB. Today there are two cables connecting the radio to each antenna, a long cable of 30 m and a short cable of 6 m. For UHF, the long cable has a measured loss of 7 dB and the short cable with the overlap is expected to give 1 dB loss in addition. A new, longer cable replacing the two cables is desired, and with that it is expected a reduction in the loss with 1 dB.

**Propagation loss** The estimate for propagation loss includes only free space loss and polarization mismatch loss, which are the same as earlier. The polarization mismatch loss is due to the linear polarization in the dipole antenna in the satellite and the circular polarization at the ground station. Atmospheric losses due to attenuation by atmospheric gases are small for UHF, i.e. in order of magnitude of 0.1 dB for low elevations at 450 MHz[27], and will therefore be included in the fading margin. Due to the uncertain nature of the ionospheric scintillation, it is not included as an own section under propagation loss. The ionospheric scintillation however, is expected to have effect on the attenuation of the signal. Peak-to-peak fluctuations rarely exceed 10 dB at high latitude regions, not even during solar maximum[10]. By contrast, the largest fluctuations only happen in a small percentage of the time, and since communication on each pass is not vital, some passes without reliable transmission is acceptable.

**The ground station and the satellite as a receiver** Gaussian Minimum Shift Keying (GMSK) is the selected modulation method, and it requires a minimum  $E_b/N_0 = 13$  dB for a reliable transmission.

The latest link budgets are based on the above calculations and assumptions.

Downlink budget for 437 MHz				
<b>Common parameters</b>		Value	Unit	
Carrier frequency		437000000,00	[Hz]	
Carrier wavelength		0,69	[m]	
Speed of light		300000000,00	[m/s]	
Earth radius		6378000,00	[m]	
Pi		3,14		
Boltzmann's constant		1,38E-023	[J/K]	
		-228,60	[dB/K/Hz]	
Baud rate		9600,00	[baud]	
<b>Noise properties</b>				
Noise bandwidth		15000,00	[Hz]	
System noise temperature		180,00	[K]	
Noise power (referred to receiver input)		-164,29	[dBW]	
Downlink budget			Best case	Worst case
<b>Orbit parameters</b>	Value	Unit	Value	Unit
Elevation	90,00	[deg]	5,00	[deg]
Orbit height	400000,00	[m]	800000,00	[m]
Maximum distance	400000,00	[m]	2783851.47	[m]
<b>Transmitter - Ground Station</b>				
Transmitted power	1,00	[W]	0,30	[W]
	0,00	[dBW]	-5,23	[dBW]
Transmission line loss in satellite	8,00	dB	8,00	dB
Antenna gain	2,00	[dB]	2,00	[dB]
Output RF Power (EIRP)	-6,00	[dBW]	-11,23	[dBW]
<b>Propagation losses</b>				
Free space loss	137,29	[dB]	154,14	[dB]
Polarization loss	3,00	[dB]	3,00	[dB]
Total path loss	140,29	[dB]	157,14	[dB]
<b>Receiver - Satellite</b>				
Receiver antenna gain	16,00	[dB]	16,00	[dB]
Received power	-138,29	[dBW]	-160,37	[dBW]
	-108,29	[dBm]	-130,37	[dBm]
	1,48E-011	[W]	9,19E-014	[W]
Received Eb/N0	27,94	[dB]	5,86	[dB]
Minimum Receiver Eb/N0	13,00	[dB]	13,00	[dB]
Received C/N	26,00	[dB]	3,92	[dB]
Uplink fading margin	14,94	[dB]	-7,14	[dB]

Table 2.1: Downlink budget for 437 MHz.

Uplink budget for 437 MHz				
<b>Common parameters</b>				
	Value	Unit		
Carrier frequency	437000000,00	[Hz]		
Carrier wavelength	0,69	[m]		
Speed of light	300000000,00	[m/s]		
Earth radius	6378000,00	[m]		
Pi	3,14			
Boltzmann's constant	1,38E-023	[J/K]		
	-228,60	[dB/K/Hz]		
Baud rate	9600,00	[baud]		
<b>Noise properties</b>				
Noise bandwidth	40000,00	[Hz]		
System noise temperature	210,00	[K]		
Noise power (referred to receiver input)	-159,36	[dBW]		
<b>Uplink budget</b>				
	Best case		Worst case	
	Value	Unit	Value	Unit
<b>Orbit parameters</b>				
Elevation	90,00	[deg]	5,00	[deg]
Orbit height	400000,00	[m]	800000,00	[m]
Maximum distance	400000,00	[m]	2783851.47	[m]
<b>Transmitter - Ground Station</b>				
Transmitted power	75,00	[W]	75,00	[W]
	18,75	[dBW]	18,75	[dBW]
Transmission path loss in ground station	8,00	dB	8,00	dB
Antenna gain	16,00	[dB]	16,00	[dB]
Output RF Power (EIRP)	26,75	[dBW]	26,75	[dBW]
<b>Propagation losses</b>				
Free space loss	137,29	[dB]	154,14	[dB]
Polarization loss	3,00	[dB]	3,00	[dB]
Total path loss	140,29	[dB]	157,14	[dB]
<b>Receiver - Satellite</b>				
Receiver antenna gain	2,00	[dB]	2,00	[dB]
Received power	-119,54	[dBW]	-136,39	[dBW]
	-89,54	[dBm]	-106,39	[dBm]
	1,11E-009	[W]	2,30E-011	[W]
Received Eb/N0	46,02	[dB]	29,17	[dB]
Minimum Receiver Eb/N0	13,00	[dB]	13,00	[dB]
Received C/N	39,82	[dB]	22,97	[dB]
Uplink fading margin	33,02	[dB]	16,17	[dB]

Table 2.2: Uplink budget for 437 MHz.

## 2.2 Comments

The worst case of the downlink budget states an insufficient  $E_b/N_0$  to have a reliable transmission for the lowest elevation angles. However, the whole visible time is probably not used for communication as the communication is low data rate telemetry. As seen when using equation 2.4 in [3], the visible time for minimum elevation 5 degrees varies between 7.9 minutes to 12.7 minutes for orbit heights 400-800 km. The satellite will have an orbit period about 1.5 hour (depending on the orbit height). This gives that the satellite have 16 passes in twenty-four hours. Most of these passes are visible from Svalbard, as a polar orbit is assumed. From visible time simulations in [11], it is seen that 4-5 passes are visible at Trondheim and 9 passes are visible from Svalbard in twenty-four hours. So it is not critical that there is communications with NUTS on each pass. Furthermore, a proposed national collaboration between student satellite ground stations at universities will increase the visible time. Additionally if the ground station take part in the worldwide GENSO network[13], NUTS can receive telemetry and/or other data even when the satellite is not visible from Norway.

The process of deciding on a link budget is a continuous process, and some parameters are only an estimate until the satellite system design is more clarified. An example of this is the system noise temperature and antenna temperature. Furthermore, the orbit height is not known until a late stage in the project, when it is known which rocket launch NUTS can hitchhike with.

## Chapter 3

# Antenna system

The complete antenna system consists not only of the antennas, but also of the system surrounding it. A sketch of the antenna system is displayed in Figure 3.1.

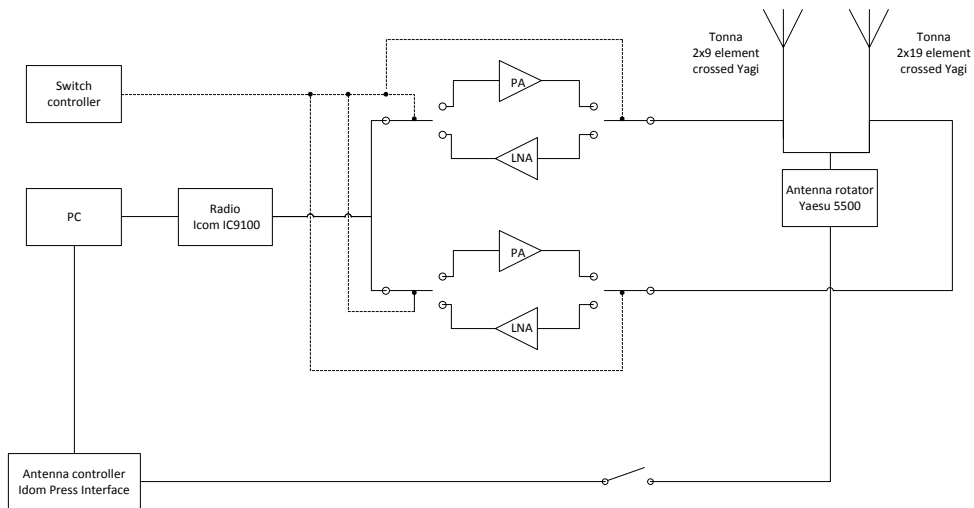


Figure 3.1: Sketch of the antenna system[3].

At this time there is no Low Noise Amplifiers (LNA) or Power Amplifiers (PA), they can be added later to achieve a better SNR.

In Figure 3.2, the two Yagi Uda antennas can be seen. On the left hand side

is the bigger Yagi Uda antenna for 145 MHz and on the right hand side is the smaller Yagi Uda antenna for 437 MHz. The intention here is that the spot for the 437 MHz antenna is interchangeable with the off-the-shelf Yagi Uda antenna and in-house designed helical antenna.



Figure 3.2: The antenna rig at the roof of Electro Block D building at NTNU with two crossed Yagi Uda antennas mounted.

The antennas are mounted on a mast on the roof of Electro Block D at Gløshaugen Campus. Figure 3.3 shows the 5th floor of the Electro Block D building.

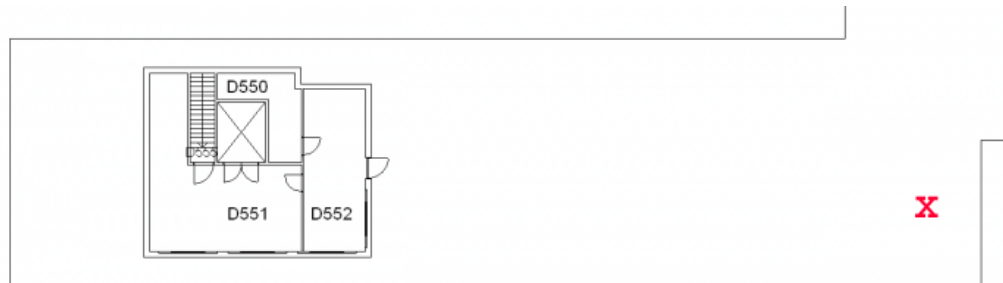


Figure 3.3: Map of the 5th floor of the Electro Block D building[12]. To the right is the indoor part of the ground station containing the radio, steering controller of the antenna rig and the computers. The red cross indicates where the antennas are mounted on the roof.

## Chapter 4

# Interface between the antenna and the ground station system

The orientation of the helical antennas when mounted on the antenna mast is controlled by two rotators. The beam attached to the antenna is steerable 360 degrees in azimuth and 180 degrees in elevation. The system is controlled by Yaesu G-5500 Elevation-Azimuth Dual Controller, which can be run by software. The radio used in the ground station is an Icom IC-9100, and the helical antennas should be used with this radio when antennas are constructed. See Figure 4.1 for an overview of the radio, rotator controller, computer interface of the rotator controller and the computer that connects all the sub sections.

### 4.1 Different tracking systems

To ensure a connection between the ground station and the satellite, some kind of signal acquisition and tracking must be employed. The tracking system will be activated when the received signal is large enough. To locate the satellite, two search methods can be used: automatic search with automatic tracking or manual search in expected satellite position[14]. The tracking itself can be automatic, programmed, manual or any combination of these. Automatic tracking are closed loop control system. In program tracking the antenna is moved in position by prediction of position. In manual tracking the antenna is moved by manual commands. Manual tracking also works as an important back up system if the automatic or program tracking fails.

Mono pulse, step pulse and conical scan are all examples of auto track systems. In the mono pulse technique, the position error is acquired from simultaneous lobing of the received signal and can be a comparison of phase, amplitude or both. In step pulse tracking, the error in position is acquired from amplitude

sensing. This technique is based on moving the antenna in small steps until the received signal is maximized. In conical scan the antenna is switched between two positions. The received echo will be equal in magnitude if the target is located between these two positions[14].



Figure 4.1: To the left: Icom IC-9100 radio and Yaesu G-5500 Elevation-Azimuth Dual Controller. To the right: Yaesu GS-232B Computer Controller with Switching Power Supply, Icom IC-PCR1500 radio for downloading signals from weather satellites and a computer with appropriate software for communication and tracking.

## 4.2 Tracking programs

There are several possibilities when choosing tracking programs for the ground station; one can choose between freeware or professional programs for purchase. The programs of interest include satellite tracking and/or prediction, in addition to a graphical interface. Only a few of the programs include antenna steering and radio tuning, or the possibility of adding software to do this. AMSAT and DXZone (DXZone is an internet resource dedicated to Amateur Radio community) presents extensive lists of various programs<sup>1</sup>, however, it has been chosen to use WXtrack for the ground station at NTNU, at least as a starting point. This program was recommended by Academic Radio Club (ARK) at Samfundet<sup>2</sup>. WXtrack supports antenna steering and as an extra facility for registered

<sup>1</sup>For overview of various tracking programs, see AMSAT's web page: <http://www.amsat.org/amsat-new/tools/software.php#shareware> and DXZone's web page: [http://www.dxzone.com/catalog/Software/Satellite\\_tracking/](http://www.dxzone.com/catalog/Software/Satellite_tracking/)

<sup>2</sup>Samfundet or the Student Society is an organization owned and run by students in Trondheim.

or paid users WXtrack also supports radio control. WXtrack predicts the orbit of a satellite by downloading Kepler parameters online, and predicting where the satellite will surface on the horizon. The antennas are then pointed in that direction, and will start receiving if the predicted position is correct. The antenna rotators will move the antennas in the predicted path of the satellite and the frequency shift due to Doppler is changed automatically. WXtrack is an example of programmed tracking. A more advanced auto track can be implemented at a later stage of the project if found necessary.

## Chapter 5

# Local environment

### 5.1 Horizon outline

To be able to know when the satellite theoretically is visible from the antenna rig, a horizon outline can be made for the local area around the ground station. This is done by equipment not usually operated by an electronic engineer, a theodolite. The theodolite is a telescope that is rotatable in both azimuth and elevation. It measures angles in azimuth and elevation, which can be used to produce a map of the local horizon outline. The theodolite is shown in Figure 5.1.



Figure 5.1: A theodolite.

With loan and guidance of a theodolite from the Department of Civil and Transport Engineering, the horizon outline displayed Figure 5.2 and Figure 5.3 was made from the position on the roof close to where the antennas are placed.

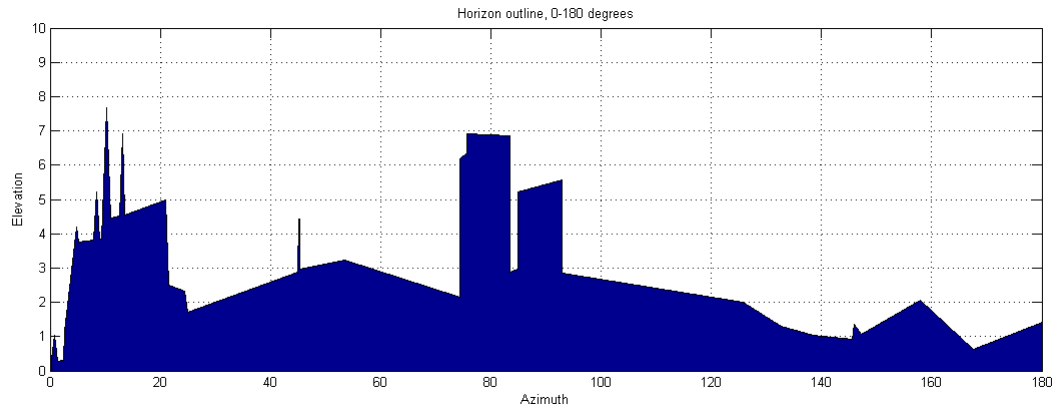


Figure 5.2: The horizon outline from 0 to 180 degrees.

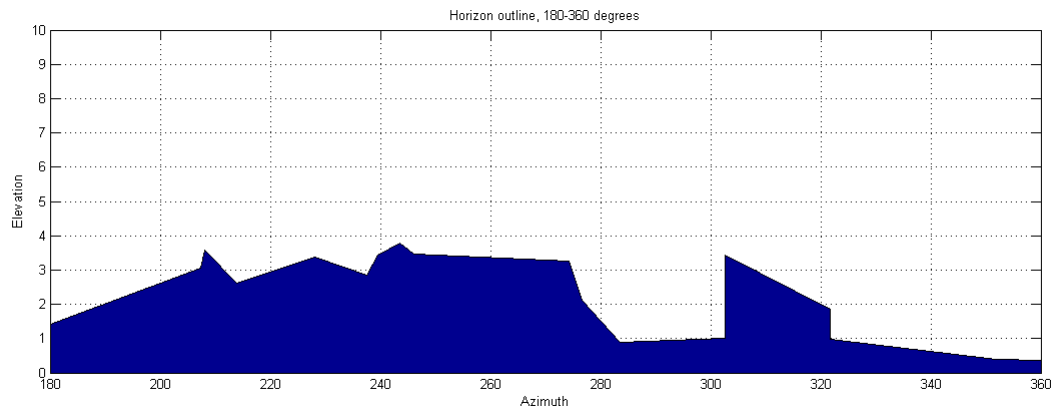


Figure 5.3: The horizon outline from 180 to 360 degrees.

From Figure 5.2 and Figure 5.3 it can be seen that most of the time there is only a 3 degree difference between the true and the visible horizon, which means that the antennas on the roof have a very good visibility in elevation for most of the azimuth angles.

It should be noted that measurements done with the theodolite are not perfectly accurate, mainly of two reasons. Firstly, the measurements are not done at the exact point where the antennas are mounted, but about a meter to the side and a couple of meters lower than the antennas. Secondly, the intersection between where the first and the last point is measured is not a perfect match. It is assumed that the equipment was moved slightly during the measuring period, and since the theodolite is very accurate, a very small displacement of the equipment will be noticeable in the resulting horizon outline. The stitching point in question can be seen on the right hand side in Figure 5.3, where the building of the roof lab has a sloping wall. In addition to these two errors, a recognizable horizon outline can be seen. The reason for not repeating the measurements is because the horizon outline does not need to be very accurate. The steerability of the antenna rig rotators only has an accuracy of about 2-3 degrees, but the horizon outline presented gives a good indication of when the satellite should be visible.

## 5.2 Wind

The antennas should tolerate stress from typical Norwegian weather. In addition to wind, this also includes heating on warm, sunny days and cooling with snow and ice on winter days. The rain might be slightly acidic, which leads to corrosion of some metals, but not so often in copper alloys. Only wind is considered in this section.

Wind load on a structure is defined as how much pressure the wind forces on the given structure. There are several reasons why calculation of wind load is important in antenna design,

- Overall strength (for safety)
- Loads on rotators
- Freedom from oscillations
- Pointing accuracy
- Distortion of the antenna structure

The first bullet point in is concerning safety, and ensures that with proper design, the antenna will stay in place even on the windiest day of the year. The four last bullet points describes that the wind can undermine the performance of the antenna.

Wind pressure can be calculated as

$$\text{Wind pressure} = 0.5 \cdot \rho \cdot v_{wind}^2 \quad (5.1)$$

where  $\rho$  is the density of air, which is approximately  $1.2 \text{ kg/m}^3$ , and  $v_{wind}$  is the wind speed. Wind force can roughly be calculated as

$$\text{Wind force} = \text{Area} \cdot \text{wind pressure} \cdot \text{drag coefficient} \quad (5.2)$$

With a wind speed of 15 m/s, the wind pressure is 135 N/m<sup>2</sup>. If the helical antenna is assumed to take form as a cylinder with circumference 0.8 m and height 1.37 m<sup>1</sup>, the wind is assumed to hit half of the surface at the time, and the drag coefficient is set to unity, then the wind force will be about 74 N. This is a very simplified calculation of the wind force, since the antenna structure is not a flat sheet with the pressure evenly distributed. Also, the drag should be included. The wind load for the different ground conductors, seen in Table 5.1, are calculated from the assumption that structures are circular, flat sheets with the area calculated from the largest diameter, the height is not included. The dimensions of the ground conductors are taken from Part II Helical antenna.

Ground conductor / dimension	Diameter (largest)	Area	Wind load
Flat	0.515 m	0.21 m <sup>2</sup>	28 N
Cupped	0.685 m	0.37 m <sup>2</sup>	50 N
Truncated cone	1.716 m	2.31 m <sup>2</sup>	312 N

Table 5.1: The wind load for the different ground conductors.

The wind load for the antenna with each ground conductor are calculated to be 103 N, 125 N and 387 N for the flat, cupped and truncated cone ground conductor, respectively. This is compared to the wind load for the helical antennas that ARK at Samfundet uses. The antennas at Samfundet are named WiMo 70-2 and they operate at the same frequency as one of the telemetry links as the NUTS project, namely 437 MHz. WiMo 70-2 has 14 turns, is 2.7 meters long and the technical data states that this design have a wind load of 225 N. WiMo 70, however, is more similar to the helical antenna designed in this thesis, since WiMo 70 has 7 turns and is 1.5 m long. WiMo 70 has a wind load of 125 N. This is in the same order of magnitude as for the flat ground conductor and the cupped ground conductor. The truncated cone ground conductor, however, presents a very high wind load, which is expected from the significantly larger size.

To achieve less wind resistance, all of the ground conductors could decrease their surface area by making perforation in the metal, or even make a mesh by thin metal wires.

Moreover, a more precise wind load estimate can be achieved from measuring on the full scale antenna in a wind tunnel.

<sup>1</sup>These values are taken from the final design in Part II Helical antenna.

## Part II

# Helical antenna

# Chapter 6

## Theory

In this chapter some general theory about helical antennas are introduced, the theory are divided in three parts. First comes a section with the classic physical structure and some aspects of the most relevant electrical and mechanical properties are highlighted. Additionally the effects of the ground conductor are presented. Second comes a small section introducing alternative physical structures. The last section presents various parameters. The first of these parameters are used for describing the performance of the antenna, like gain and polarization. Second comes parameters that relates to an antenna array, which also can influence the performance. In the end more general parameters that are very relevant for this thesis are presented, like input impedance and voltage standing wave ratio.

### 6.1 Classic physical structure

A helical antenna is a conducting wire wound in the shape of a screw as illustrated in Figure 6.1.

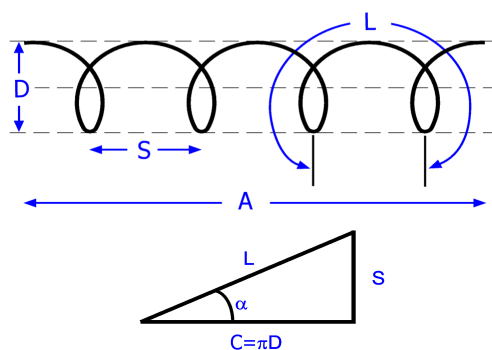


Figure 6.1: Helical antenna structure[1]

Parameters:

- L = length of a loop
- D = diameter of one loop
- C = circumference of the helical
- S = spacing between two loops (center to center)
- A = total axial length
- n = number of loops
- $\alpha = \text{pitch angle} = \arctan\left(\frac{S}{\pi D}\right)$
- d = diameter of the conductor

To obtain the desired radiation properties for a given wavelength, the parameters listed above must be adjusted. Additionally, the conducting wire can be made of various materials. Electrical and mechanical properties must be evaluated. Since the material possibilities are limited, only the most relevant material properties are included. In the end, availability and price must also be evaluated.

### 6.1.1 Electrical properties

The electrical properties of a material describe how well the material conducts and how much loss there is under certain conditions.

Conducting materials have the electrons in the outermost shell of the atom more loosely bound than other materials such as semiconductors and insulators. The parameter that is used to measure the ability to conduct is called conductivity,  $\sigma$ , which is a product of electron mobility,  $\mu_e$ , and charge density of the drifting electrons,  $\rho_e$ , see Equation 6.1.

$$\sigma = -\rho_e \mu_e A / V_m = -\rho_e \mu_e S / m \quad (6.1)$$

A good conductor has a high conductivity (or low resistivity). Antennas are often made of copper or aluminum, at average low-frequency in room temperature they have conductivity  $\sigma_{Cu} = 5.80 \times 10^7 \text{S/m}$  and  $\sigma_{Al} = 3.54 \times 10^7 \text{S/m}$  respectively[17]. However, these values are dependent of the purity of the metal, temperature and frequency. It is said that a good conductor has the following conductivity,  $\sigma \gg \omega \varepsilon$ , where  $\omega$  is the angular frequency and  $\varepsilon$  is permittivity. On the other hand, a good insulator has  $\sigma \ll \omega \varepsilon$ [17]. Silver has better conductivity than both copper and aluminum, but is not an alternative because of the high cost.

### 6.1.2 Mechanical properties

There are also mechanical considerations for an antenna. Rigidity, elasticity and weight should be taken into consideration before a decision is made.

Rigidity and elasticity is of interest since the antenna should be shaped as a screw, but at the same time tolerate stress from wind. There are different ways to classify rigidity and elasticity of a material, the most relevant here is Young's modulus. Young's modulus is the ratio between tensile stress and strain, denoted Pascal [ $Pa$ ], and describes relative elastic stiffness for a material[18]. The Young's modulus is roughly 70 GPa for aluminum and 110 GPa for copper[18]. This shows that copper is more rigid than aluminum.

When it comes to weight consideration, aluminum is the better choice than copper since it has lower density. Aluminum has  $2.70\text{ g/cm}^3$  and copper has  $8.95\text{ g/cm}^3$ . These values are for the metals in pure form, but it is expected that aluminum and copper alloys will roughly have the same weight as their pure version.

### 6.1.3 Ground conductor

A design goal is to have large gain, and with proper shaping of the ground conductor, the gain of a helical antenna can be enhanced by reducing backfire radiation. The current distribution of a helical antenna decreases rapidly during the first two turns of the antenna, and then remains approximately constant for the rest of the turns before going to zero in the end. The first region with rapid decrease is called the C region or exciter region, where phase velocity<sup>1</sup> and phase progression is almost the same as in free space. The second region is named the S region or surface wave region, and has almost constant current[25]. The current distribution in the exciter region contributes to the backfire radiation, and this backfire radiation could be reduced with proper choice of ground conductor.

The most common method to feed an helical antenna is to place it over a ground conductor and feed the antenna with a coaxial input or micro strip line[25]. The ground conductor can have different sizes and shapes, and this will influence the performance of the antenna[39]. It is shown with numerical analyzes that a ground conductor transform backfire radiation into forward radiation if the ground conductor has a size comparable to the wavelength[19]. A smaller ground conductor radius gives more backfire radiation, and thus a minimum size should be used.

It is desired to have a large gain in this design, and with proper size and shape of the ground conductor, the antenna gain could be enhanced with as much as 4 dB[20]. Three ground conductors are of special interest, a flat conductor like a square or circle, a cylindrical cup and a truncated cone. These are shown in see Figure 6.2.

---

<sup>1</sup>Phase velocity is the propagation velocity of an equiphased front[17].

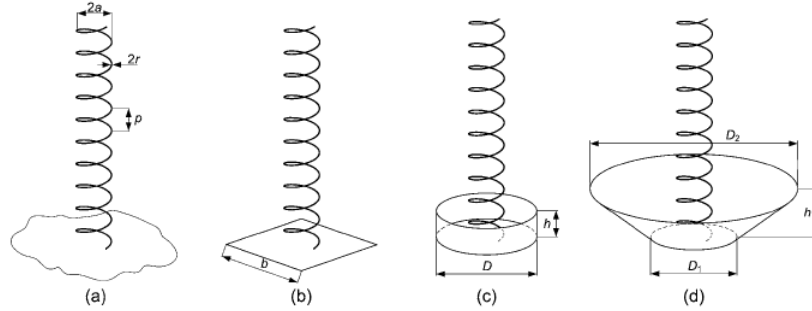


Figure 6.2: Different ground conductor opportunities for a helical antenna; (a) infinite ground plane, (b) square conductor, (c) cylindrical cup, and (d) truncated cone[20].

## 6.2 Other possibilities for physical structure

The helical antenna structure does not need to be as shown in Figure 6.1. It is also possible to vary the circumference of each loop as in a hemispherical and a spherical helical antenna. This is shown in Figure 6.3.

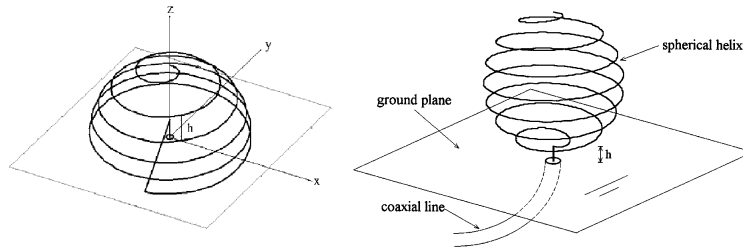


Figure 6.3: To the left: hemispherical helical antenna[21], to the right: spherical helical antenna[22].

Both the antenna structures in Figure 6.3 shows intriguing design possibilities, however this thesis continues the work on conventional helical antennas presented by the former NTNU students Mireia Oliver Miranda[1] and Laurea Magistrale[2].

## 6.3 Characterization of antenna and antenna system

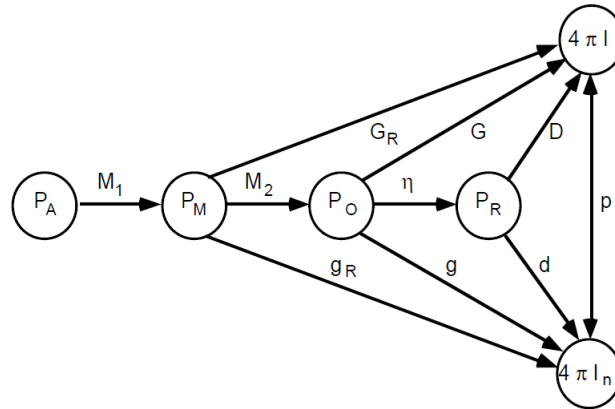
The performance of the antenna, which includes the description of how the radiating waves behaves in space and in relation to the antenna, is described by several parameters. To understand how to optimize an antenna, which limits there are, and the compromises that must be made in the design process, a good understanding of these parameters is essential.

### 6.3.1 Directivity

From IEEE Standard Definitions of Terms for Antennas, directivity has the following definition, “The ratio of the radiation intensity in a given direction from the antenna to the radiation intensity averaged over all directions.”[38] Further, there is a definition for partial directivity, which corresponds to a given polarization, “In a given direction, that part of the radiation intensity corresponding to a given polarization divided by the total radiation intensity averaged over all directions.”[38] For a helical antenna made out of a good conductor, the losses can be small enough so that the directivity and gain is roughly equal[25].

### 6.3.2 Gain

Gain describes the performance of the antenna with not only direction consideration, as directivity, but also efficiency. There are different ways to describe the gain of an antenna. IEEE Standard Definitions of Terms for Antennas explain four types; (absolute) gain, partial gain, realized gain, and partial realized gain[38]. For absolute gain in a given direction the following applies, “The ratio of the radiation intensity, in a given direction, to the radiation intensity that would be obtained if the power accepted by the antenna were radiated isotropically.”[38] Partial gain however, only includes the gain that corresponds to a given polarization, which means that “In a given direction, that part of the radiation intensity corresponding to a given polarization divided by the radiation intensity that would be obtained if the power accepted by the antenna were radiated isotropically.”[38] So if there are two orthogonal polarizations, the sum of these two partial gains would be the total gain[38]. Realized gain is “The gain of an antenna reduced by the losses due to the mismatch of the antenna input impedance to a specified impedance”[38] Partial realized gain is a combination of partial gain and realized gain[38]. To better comprehend the differences between these gains, see Figure 6.4.



$P_A$ = power available from the generator	$\eta$ = radiation efficiency
$P_M$ = power to matched transmission line	$G_R$ = realized gain
$P_O$ = power accepted by the antenna	$G$ = gain
$P_R$ = power radiated by the antenna	$D$ = directivity
$I$ = radiation intensity	$g_R$ = partial realized gain
$I_n$ = partial radiation intensity <sup>†</sup>	$g$ = partial gain
$M_1$ = impedance mismatch factor 1	$d$ = partial directivity
$M_2$ = impedance mismatch factor 2	$p$ = polarization efficiency

Figure 6.4: Gain and Directivity Flow Chart. All partial quantities corresponds to a specified polarization.[38]

The gain that is stated in the link budget is the absolute gain, hence the additional losses due to impedance and polarization mismatch are not included.

### 6.3.3 Antenna efficiency

Antenna efficiency take losses at input terminals and within the antenna structure into account. The total efficiency is the product of reflection (mismatch) efficiency, conduction efficiency and dielectric efficiency, where the two last one are usually taken as one parameter since they are hard to separate when measured[24]. The most relevant in this thesis is to increase reflection efficiency by impedance matching.

### 6.3.4 Polarization

From IEEE Standard Definitions of Terms for Antennas, polarization can be understood in three related ways:

- 1) To a field vector at some point in space
- 2) To a plane wave
- 3) To an antenna

Since these three interpretations are related, the interpretation of polarization for a field vector at some point in space and for a plane wave is part of the explanation of polarization of an antenna. “The polarization to a field vector specifies the shape, orientation and sense of the ellipse that the extremity of the field vector describes as a function of time.”[38] For polarization of a plane wave the following applies, “In a single-frequency plane wave a specified field vector has the same polarization at every point in space”[38] Lastly, for an antenna, the term polarization is used as following “The polarization of an antenna in a given direction is that of the plane wave it radiates at large distances in that direction”[38]

The polarization can be described as linear, circular or elliptical. Linear and circular polarization can be seen as special cases of elliptical polarization. The linear case is when the electrical field vector at a point in space is a function of time points along a line[24]. This can be illustrated with either  $E_{y0}$  or  $E_{x0}$  equal zero in Figure 6.5, or when two orthogonal linear components are either in phase or 180 degrees out of phase[24]. The linear polarization can be described as either horizontal or vertical.

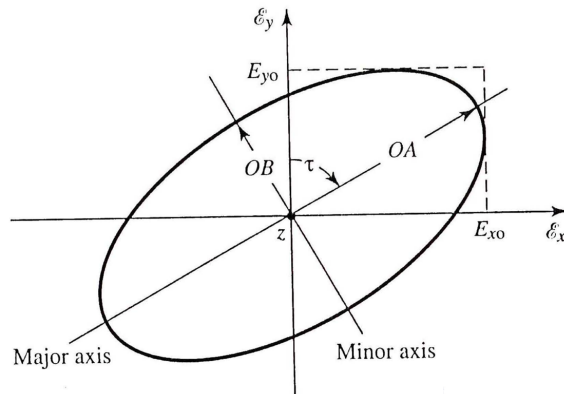


Figure 6.5: Polarization of a wave[24].

Circular polarization is achieved when there are two orthogonal linear components with same magnitude and time-phase difference of odd multiples of 90 degrees[24]. The circular polarization can be left-handed (LHC) or right-handed (RHC), which describes the direction the extremity of the field vector rotates. For a plane wave that is viewed in the propagation direction, clockwise rotation of the field vector corresponds to LHC. And opposite, counterclockwise rotation of the field vector corresponds to RHC[38]. LHC and RHC are orthonormal and the desired LHC or RHC polarization is denoted co-polarization and the unwanted one is denoted cross-polarization[26]. The mix of co-polarization and cross-polarization determine the quality of the circular polarization.

When the polarization is neither linear or circular, the polarization is elliptical and the field has two linear orthogonal components. If the magnitudes of

the components are the same; the time-phase difference cannot be odd multiples of 90 degrees, since that would give circular polarization. If the magnitudes of the components are different, the time-phase difference can not be 0 degrees or multiples of 180 degrees, since that would give linear polarization[24].

A linearly polarized wave consist of two equal but counter-rotating field components of circular polarization, and elliptical polarization consist of two not equal counter-rotating field components of circular polarization. The fact that the counter-rotating field components is not equal makes cross-polarization discrimination harder for elliptical polarization than for linear and circular polarization. So to avoid the need of being very accurate with the phase, elliptical polarization is usually not preferred for satellite communication, and hence not used in this thesis.

For a satellite that passes over a ground station, there will be a slight shift of the polarization if the polarization is linear, because the tilt relative to the electric field of the earth will vary. This shift in polarization will require polarization tracking of the signal. If the polarization tracking is not accurate, there will be polarization loss[27]. Consequently linear polarization is not preferred for the ground station antennas.

Both right-handed and left-handed polarization can be utilized, and at bigger ground station as Andøya Rocket Range[28], the ground equipment can receive both at the same time.

Different kinds of polarization is achieved by adjusting the physical structure, and in some cases the orientation of the antenna. To get circular polarization of a helical antenna, the ratio between the circumference of one loop and the wavelength at the center frequency must be in the interval given in Equation 6.2.

$$3/4 < C/\lambda < 4/3 \tag{6.2}$$

Additionally, the spacing between to loops must approximately be a quarter of the wavelength, see Equation 6.3.

$$S \approx \lambda/4 \tag{6.3}$$

Lastly the pitch angle should be between 12 and 14 degrees, and there should be more than three loops on the helical antenna[24]. The orientation of a helical antenna does not influence the polarization when it is circularly polarized.

### 6.3.5 Radiation pattern

Radiation pattern is defined by IEEE Standard Definitions of Terms for Antennas as: “The spatial distribution of a quantity that characterizes the electromagnetic field generated by an antenna.”[38]

The quantities that characterize the electromagnetic field could be amplitude, phase, polarization, power flux density, radiation intensity, field strength, etc. The field can be divided into three regions: reactive near field, radiating near field and far field. See Figure 6.6.

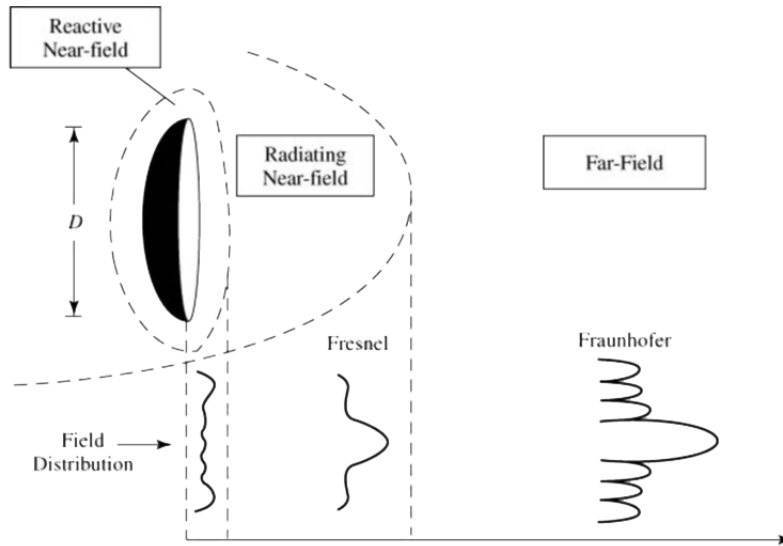


Figure 6.6: Illustration of typical changes in amplitude pattern from near to far field[24].

The boundaries that separate these regions are not definite, but in most cases they are described as follows. The reactive near field is from the surface of the antenna to the distance  $R < 0.62\sqrt{D^3/\lambda}$ , where  $D$  is the biggest dimension of the antenna and  $\lambda$  is the wavelength. The radiating near field is limited by the reactive near field as inner boundary, and  $R < 2D^2/\lambda$  as outer boundary. When the maximum dimension  $D$  is small compared to the wavelength there may not be any separation between these two near fields[24]. The far field inner boundary is  $R < 2D^2/\lambda$  and outer boundary has no limit. Far field is defined as “That region of the field of an antenna where the angular field distribution is essentially independent of the distance from a specified point in the antenna region.”[38]

When it comes to satellite communication, the ground station and the satellite are definitively in each others far field. However, when antenna measurements are done at ground level, if for instance a helical antenna where to be tested, the distance between the antenna and the receiver must be selected in such manner that the measurements are done in the far field region.

The radiation pattern consist of lobes of various sizes, the direction with the maximum radiation intensity is known as the major lobe or the beam of the antenna. In this major lobe, the half power beam width (HPBW) is measured. The HPBW is the angle between the two direction where radiation intensity have decreased to half of the maximum radiation. This angle is inversely proportional to the square of directivity or the gain, and is a useful parameter when the gain is difficult to measure.

A helical antenna can radiate both in the axial mode (also known as end-fire

mode) and in the normal mode (also known as broadside mode), see Figure 6.7. From this figure, it can be seen that an antenna that radiates in the normal mode radiates in a plane perpendicular to the axial length. In axial mode the antenna radiates along the axial length. Since the satellite can only be found in one place at one time, it is reasonable to choose the axial mode. Further, axial mode can achieve circular polarization over a wider bandwidth[24].

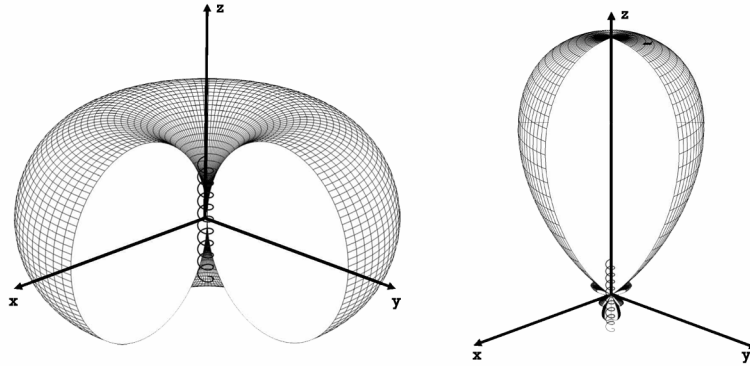


Figure 6.7: The left side of the figure shows normal mode and the right side shows axial mode[24].

There are two types of axial modes; the ordinary and Hanson-Woodyard. The two modes have different relative phase velocity<sup>2</sup>, and the Hanson-Woodyard mode has more directive capabilities. When the circumference is within the circular polarization criteria, see Equation 6.2 in the Polarization section, the relative phase velocity of the wave traveling along the helical antenna is close to that of the Hanson-Woodyard[24], and thus this application should operate with Hanson-Woodyard axial mode.

### 6.3.6 Antenna array

Gain of an antenna array is dependent of the design of one helical antenna and the number of helical antennas in an array[39]. When it comes to weather considerations, it might be wiser to have a shorter helical antenna, as it will experience less stress from wind. To achieve the desired gain, an array of shorter antennas can replace one long antenna. The total gain can be calculated by adding the gain of each element. However, there are five parameters that influence the performance of the antenna array, and then also might influence the total gain. These parameters are[25]:

- Geometry (the arrangement of the elements)
- Distance between each element

<sup>2</sup>Relative phase velocity is the ratio between the velocity which the wave travels along the helical wire and wave velocity in free space[24].

- Amplitude current excitation of each element
- Phase excitation of each element
- Radiation pattern of each element

### 6.3.7 Input impedance

The input impedance of an antenna is “The impedance presented by an antenna at its terminals”[38], and is usually a complex value. The impedance at the antenna terminals should be matched at the feeding point. To optimize the amount of power that is sent from the transmission line to the antenna, some kind of matching device should be used between the transmission line and the antenna; an antenna tuner. The ground station’s radio is an Icom IC-9100, and it has an input impedance of  $50 \Omega$ [8].

### 6.3.8 Scattering parameters

Scattering parameters, usually arranged in a matrix, the [S] matrix, describes the matching of a network by relating the incident voltage waves on the port with those reflected from the port[23]. For a two port, the scattering matrix has four parameters, as seen below.

$$\begin{matrix} S_{11} & S_{12} \\ S_{21} & S_{22} \end{matrix} \quad (6.4)$$

where  $S_{11}$  represents the reflection at the input port,  $S_{12}$  and  $S_{21}$  represents the transmission from port 2 to 1 and opposite and  $S_{22}$  is the reflection at port 2. The scattering parameters can be represented in a Smith Cart<sup>3</sup> for an useful visualization.

### 6.3.9 Voltage standing wave ratio

Voltage Standing Wave Ratio (VSWR) is the ratio between incident and reflected wave in the transmission line, which together produce a standing wave, see Equation 6.5[26].

$$VSWR = \frac{V_{max}}{V_{min}} = \frac{1 + |\Gamma|}{1 - |\Gamma|} \quad (6.5)$$

where  $\Gamma = \frac{Z_A - Z_0}{Z_A + Z_0}$ ,  $Z_A$  is the antenna impedance and  $Z_0$  is the characteristic impedance. The VSWR therefore describes to which degree the system is impedance matched, and with that the system’s reflection efficiency. Ideally the VSWR should be 1, but to have  $VSWR < 2$  in the widest possible frequency range is acceptable[29].

---

<sup>3</sup>A Smith chart is a graphical aid used for transmission lines and matching networks.

### 6.3.10 Return loss

The difference between the available power from the generator and the power absorbed by the load, in this case the antenna, is denoted return loss. The return loss is defined as

$$RL = -20\log|\Gamma| [dB] \quad (6.6)$$

where  $\Gamma$  is the reflection coefficient.  $\Gamma = 0$  represents no reflected power and  $\Gamma = 1$  represents total reflection. This leads to  $RL = \infty$  dB for a matched load[23].

## Chapter 7

# Antenna design and simulation

The preliminary antenna design is determined by the requirements given in the antenna theory and the newly revised link budget.

### 7.1 Preliminary antenna design

When it comes to antenna design there is sometimes a difference between the computed results from formulas given in acknowledged antenna literature, and what is measured on an actual structure. A method to verify the simulation is to compare computed results with measured results. Some work has been already done in this verification field, see [29] by Djordjević, Zajić, Ilić and Stüber. This article gives extensive comparison of computed and measured results for helical antennas. Since there are some difference, some adjustments must be made. Firstly, the gain is not easily calculated out of the simple gain formula given by John D. Kraus in [39]. Dr. T Emerson in [40] estimates the gain from a large number of numerical modeling calculations and states a more realistic gain, however there is still room for improvement of the gain with proper shaping of the ground conductor.

To check if the wanted design is realizable, two design curves from [29] are used. The first one compares maximal antenna gain with normalized antenna length, as seen in Figure 7.1 where the preliminary antenna design of this project is marked in red.

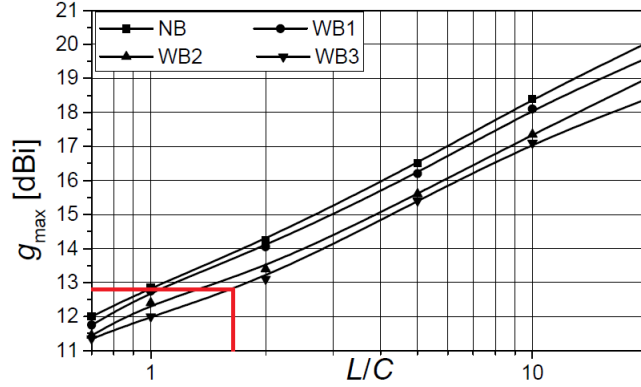


Figure 7.1: Maximal antenna gain versus normalized antenna length[29].

The figure shows that when  $L/C \simeq 1.7$ , the maximum achievable gain is about 12.8 dB for broadband applications when the total gain variation is maximum 3 dB. The maximum gain is bigger for narrower bands.

Figure 7.2 shows optimal pitch angle versus normalized antenna length with normalized wire radius as a parameter for broadband design.

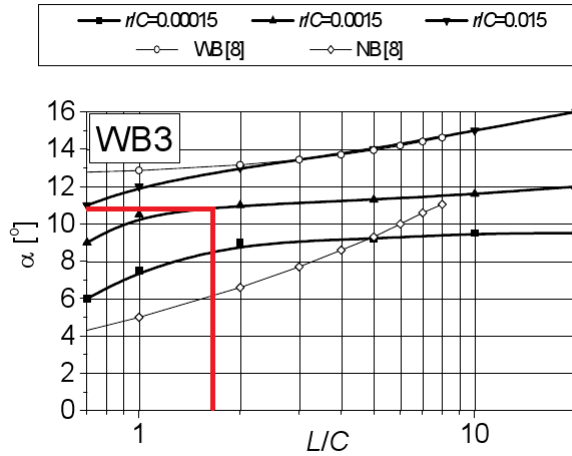


Figure 7.2: Optimal pitch angle versus normalized antenna length with normalized wire radius as a parameter for broadband design[29].

The figure shows that the chosen pitch angle is approximately one degree less than the optimum pitch angle. The reason for this choice is that the cir-

cular polarization design criteria for pitch angle also must be satisfied. Other possibilities would be a thicker wire or a shorter circumference, since this would give a higher optimum pitch angle. Secondly, the wire radius divided by the circumference is not exactly 0.0015, so the optimum pitch angle is a little lower than 11 degrees.

The design goal is to have an array of circular polarized helical antennas with 16 dB gain over the designated bandwidth, that is 435 - 439 MHz and in addition  $\pm 10$  kHz for the Doppler shift. Furthermore, the helical antennas should be made as compact as possible, which means that shorter helical antennas in an array is preferred over a single long antenna. The antenna array should also be impedance matched and have acceptable side lobes.

The first design, see Table 7.1, is based on the criteria for circular polarization given in Section 6.3 and checked against the design curves in [29].

Dimension	Abbreviation	Size	Unit
Length of a loop	L	0.8182	m
Diameter of one loop	D	0.2546	m
Circumference of the helical	C	0.8	m
Spacing between two loops	S	0.1717	m
Total axial length	A	1.3736	m
Number of loops	n	8	-
Pitch angle	$\alpha$	12.11	$^{\circ}$
Diameter of the conductor	d	0.01	m

Table 7.1: First antenna design, with only a single helical.

The diameter of the conductor is not part of the circular polarization criteria, but is chosen to be 1 cm as a starting value. The number of loops is chosen to be eight since this will give about 12.8 dB gain for each element in the antenna array. Ideally this would give about 15.8 dB gain with two elements in the array and 18.8 dB gain with four elements in the array. The optimum height of the helical antenna over the ground conductor is not known, so various distances are tested in the simulation program.

According to the theory, a flat ground conductor should be at least  $3\lambda/4$ , and the frequency 437 MHz gives that the diameter of a flat ground conductor should be bigger than 51 cm. However, a flat ground conductor might not be the best choice, so other ground conductor configurations are also taken into consideration. This includes a cupped ground conductor and a truncated cone.

## 7.2 Simulation

The simulation program used is CST MICROWAVE STUDIO<sup>®</sup> from CST STUDIO SUITE<sup>™</sup>2010, which analyzes 3D electromagnetic effects for different high frequency components including antennas[30]. The wanted results from the simulations are antenna radiation patterns and antenna gain over a frequency range,

in addition to S11, and for that purpose the transient solver was used. The transient solver calculates the development of fields through time at discrete locations and at discrete time samples[30].

### 7.2.1 Parameter variation

The dimension on the first design is given in Table 7.1 and a visualization of the structure in the simulation program is shown in Figure 7.3 .

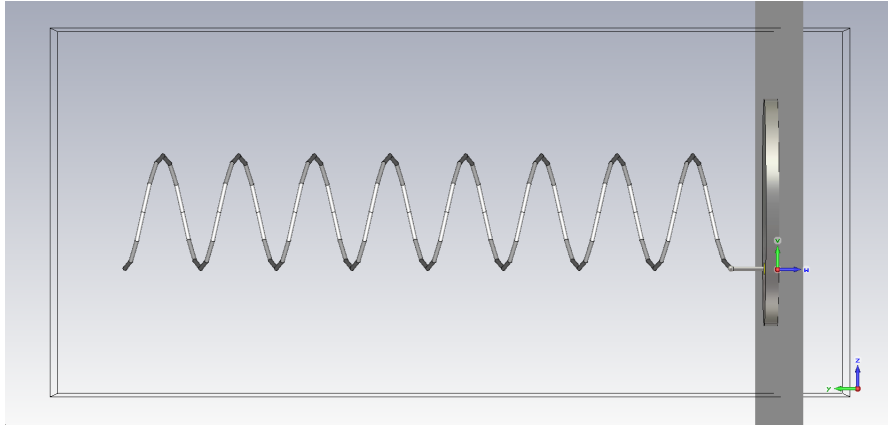


Figure 7.3: The antenna structure in CST Studio.

The figure shows that the conducting wire is made out of shorter straight cylinders with a given segmentation angle, 30 degrees. This is done to make the meshing process prior to the simulation simpler.

The optimal antenna height over the ground conductor is unknown, so different heights are tested in the simulation program. The conducting wire and the feeding point are connected together with a sphere. For heights bigger than the minimum, there is a feeding cylinder between the antenna wire and the feeding point, as shown in Figure 7.4. The conducting wire and the ground conductors are simulated as perfect electric conductors.

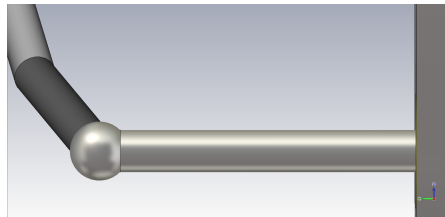


Figure 7.4: Connection between helical wire and ground conductor.

For a flat ground conductor with diameter of  $3\lambda/4 \approx 51.5$  cm, simulation re-

sults from the parameter variation can be seen in Table 7.2. Here only the gain over the given bandwidth and the 3 dB bandwidth are considered. Other parameters such as VSWR calculated, but since the antenna has not been impedance matched to  $50 \Omega$ , the VSWR ratio is not good.

Parameter	Adjustment	Gain	3 dB Bandwidth
Circumference	Larger	More	Wider
	Smaller	Less	Thinner
Feeding cylinder thickness	Larger	Almost the same	Little wider
	Smaller	Almost the same	Almost the same
Conductor thickness	Larger	More	Wider
	Smaller	Less	Thinner
Ground conductor	Larger	More	Wider
	Smaller	Less	Wider
Height over ground conductor	Larger	Less	Wider
	Smaller	More	Thinner
Number of turns	Larger	More	Wider
	Smaller	Less	Thinner

Table 7.2: Results from first parameter variation.

From Table 7.2, it is clear that some adjustments can be made to achieve more gain. The circumference and conductor thickness can be made larger, and the ground conductor can be made bigger or be given another shape. The height over the ground conductor should be lower than 7 cm, which was the first tested height. Additionally it is also possible to have more loops in the antenna. The gain curve from the first design is seen in Figure 7.5.

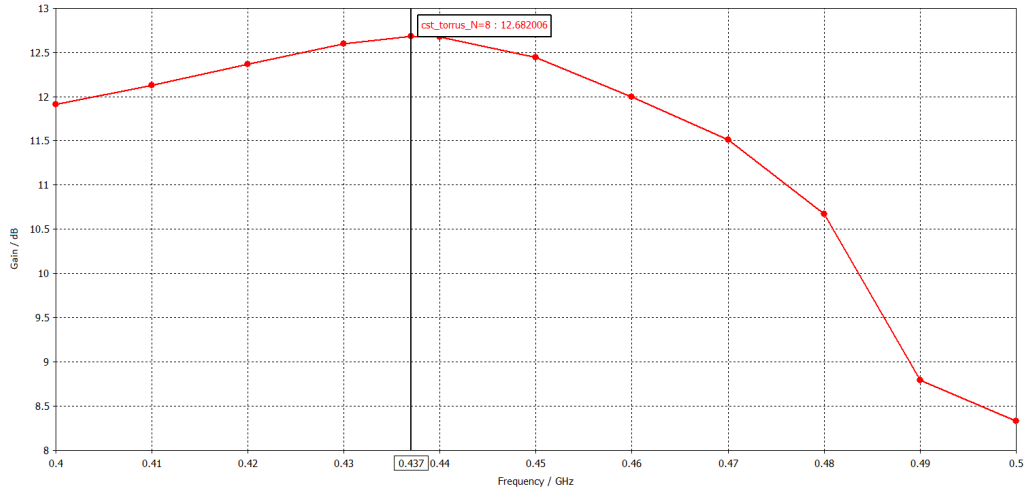


Figure 7.5: Maximum gain curve for the first design over the frequency range 400 MHz to 500 MHz, where the maximum gain at 437 MHz is marked.

As seen in Figure 7.5, maximum gain for one helical with this design is about 12.7 dB for the frequency 437 MHz. From this design, two helical antennas in an array would give about 15.7 dB gain and four helical antennas in an array would give about 18.7 dB gain.

## 7.2.2 Final design

No optimization should be made at this point, since the simulated results will not exactly correspond with the measured results. There are two reasons for this. Firstly the simulation is an approximate calculation and secondly there are measuring errors. Still some small adjustments are done to the design. The height over the ground conductor was unknown, so various distances was tested, the result was that the lowest position possible gave most gain. It was tempting to increase the wire diameter, since that gave both more gain and wider 3 dB bandwidth, however it was found that the originally 1 cm diameter would be thick enough, so the parameter was not changed. More loops gave, not surprisingly, higher gain, but since an array of shorter helical antennas are preferred over one long helical, the number of turns was not changed at first. The circumference was kept the same as a starting point, even though larger circumference would give larger gain. The reason for this is that the circular polarization criteria must be met. A large enough change in the circumference to make a considerable difference, will force either the pitch angle or the spacing between each loop outside of the circular polarization boundary.

The final design is the same as the first design seen in Table 7.1, where the height over ground conductor is about 0.7 cm, which is the radius of the sphere connecting the helical wire to the inner conductor in the coax feed. Additionally,

there are three different ground conductors that are going to be measured with the helical structure: a flat, a cupped and a truncated cone ground conductor.

The simulation result of the maximum gain for different frequencies for the flat, the cupped and the truncated cone ground conductor can be seen in Figure 7.6. The dimensions of the different ground conductors are taken as the optimum dimensions from [20], see Figure 7.7 and Table 7.3.

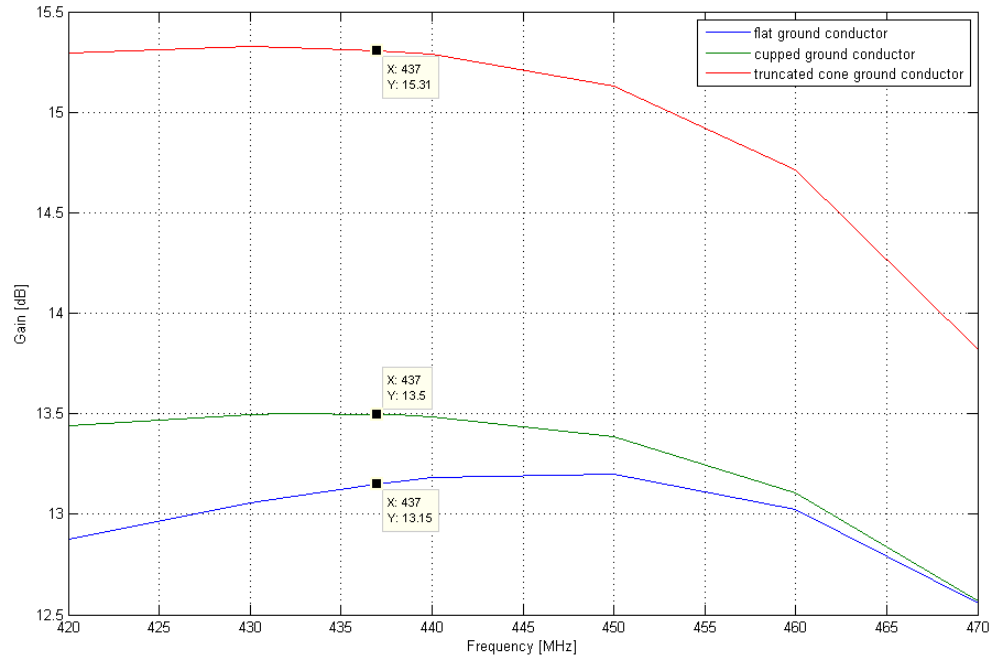


Figure 7.6: Simulated maximum gain curve for the final design over the frequency range 420 MHz to 470 MHz, where the gain at 437 MHz is marked.

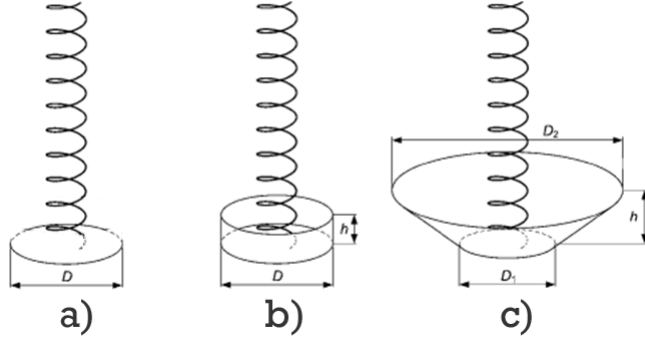


Figure 7.7: a) The flat ground conductor, where  $D$  is the diameter, b) the cupped ground conductor where  $D$  is the diameter and  $h$  is the height, c) the truncated cone ground conductor where  $D_1$  is the lower diameter,  $D_2$  is the upper diameter and  $h$  is the height.

Ground conductor / dimension	Diameter	Height	Second diameter
Flat	$\frac{3\lambda}{4} = 51.5$ cm	-	-
Cupped	$1\lambda = 68.6$ cm	$\frac{\lambda}{4} = 17.2$ cm	-
Truncated cone	$\frac{3\lambda}{4} = 51.5$ cm	$\frac{\lambda}{2} = 34.3$ cm	$2.5\lambda = 171.6$ cm

Table 7.3: Dimensions of the different ground conductors.

Table 7.4 displays a comparison between one, two and four helical antennas in an array, for the three different ground conductors.

Ground conductor / elements in the array	1	2	4
Flat	13.2 [dB]	16.2 [dB]	19.2 [dB]
Cupped	13.5 [dB]	16.5 [dB]	19.5 [dB]
Truncated cone	15.3 [dB]	18.3 [dB]	21.3 [dB]

Table 7.4: Gain comparison for simulation with different ground conductors.

See Appendix B for more simulation results. The gain for the frequency 437 MHz in 3D are seen in Figure B.1, B.2 and B.3 for the flat, the cupped and the truncated cone ground conductor, respectively. In Figure B.4 and Figure B.5 the E-field and the H-field can be displayed for the flat ground conductor at the frequency 437 MHz. The linear magnitude of the reflection at the input port is seen in Figure B.6 and the phase is seen in Figure B.7, also for the case of the flat ground conductor at 437 MHz. The remaining results are included on a CD.

### 7.2.3 Difficulties

Some difficulties were met during the simulation process. Most of the problems probably occurred in the complicated meshing process of the helical structure. A solution was to simulate an angled helical structure instead of a smooth coil. This process was made easier with another simulation program than the one originally used. So the simulation program was switched from Agilent Electromagnetic Professional (EMpro)[31] to CST MICROWAVE STUDIO.

# Chapter 8

## Final design and construction

### 8.1 Geometrical scaling

A model must be made to be able to measure inside the anechoic chamber, since the frequency of the full scale antenna is 437 MHz and the anechoic chamber only can be used for frequencies over 2 GHz. This gives a controlled measuring environment in addition to be the available measuring facility right now. Geometrical scaling will give a good approximation for the pattern measurements[24].

All linear dimensions of an antenna with pertaining ground conductor can be scaled with a factor of  $n$ , where  $n$  is usually bigger than unity. The ability to do scaling comes as a direct consequence of Maxwell's equations. See Table 8.1 for an overview of the scaled and unchanged parameters for a geometrical scale model.

Scaled Parameters		Unchanged Parameters	
Length	$l' = l/n$	Permittivity	$\epsilon' = \epsilon$
Wavelength	$\lambda' = \lambda/n$	Permeability	$\mu' = \mu$
Frequency	$f' = nf$	Impedance	$Z' = Z$
Conductivity	$\sigma' = n\sigma$	Antenna gain	$G'_o = G_o$

Table 8.1: Geometrical Scale Model[24].

The final design is a geometrical scale model, scaled down 5 times. See Table 8.2 for a dimension overview and Figure 8.1 for a picture of the model. The model is supported with a dielectric foam, Divinycell H100[32], in the core. See Table 8.3 for overview of the new dimensions of the ground conductors<sup>1</sup>.

<sup>1</sup>The dimensions of the truncated cone ground conductor was suppose to have a height of 6.9 cm and 34.3 cm as second diameter, but the bending of the aluminum to achieve the proper shape gave a height of 7.1 cm and second diameter of 33.25 cm.

Dimension	Abbreviation	Actual size	Scaled down size	Unit
Length of a loop	L	0.818	0.164	m
Diameter of one loop	D	0.255	0.051	m
Circumference of the helical	C	0.800	0.160	m
Spacing between two loops	S	0.172	0.034	m
Total axial length	A	1.374	0.275	m
Number of loops	n	8	8	-
Pitch angle	$\alpha$	12.11	12.11	$^{\circ}$
Diameter of the conductor	d	0.010	0.002	m

Table 8.2: Scaled down dimension for the model of the helical antenna.

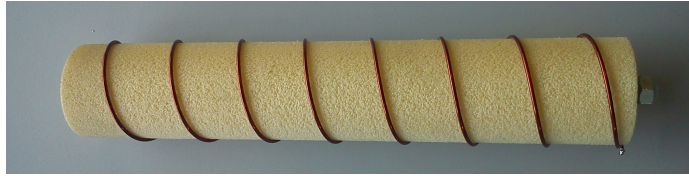


Figure 8.1: A picture of the helical antenna scale model.

The scaled down version in Table 8.2 is valid for the frequency 2.185 GHz, which has a wavelength of about 13.7 cm.

The ground conductors are all made of 2.2 mm thick aluminum alloy 5754 with hardness H32. Aluminum is chosen as the material for the ground conductors because aluminum was available in flat sheets, it is relatively cheap and aluminum has sufficiently conductivity. The helical wire is made of 0.2 cm thick oxidized copper. Copper is chosen as the conducting wire for the antenna as a result of the conductivity of copper and the fact that copper is more rigid than aluminum. Additionally was copper available as wires with various diameters.

The antenna is attached to the feed with a  $50 \Omega$  type N connector, where the connection point is hand soldered. This is a difference from the simulation where the connection point was a sphere.

Ground conductor / dimension	Diameter	Height	Second diameter
Flat	10.3 cm	-	-
Cupped	13.7 cm	3.4 cm	-
Truncated cone	10.3 cm	7.1 cm	33.3 cm

Table 8.3: Scaled dimensions of the different ground conductors.

## 8.2 Impedance matching

The antenna must be impedance matched to  $50 \Omega$ . From the simulations, the reflection coefficient (S11) for the frequency 437 MHz written in polar form, are seen in Table 8.4.

Ground conductor / Reflection coefficient	Magnitude	Magnitude	Phase
Flat	0.55	-5.2 [dB]	$-74.5^\circ$
Cupped	0.56	-5.0 [dB]	$-72.2^\circ$
Truncated cone	0.58	-4.7 [dB]	$-72.6^\circ$

Table 8.4: Reflection coefficient for the different ground conductors.

This shows that the reflection coefficient for the different ground conductors are approximately the same, as expected. Furthermore, the reflection coefficients states that around half of the input power is reflected, consequently the antenna must be impedance matched.

There are two kinds of impedance matching, one could use a matching network with lumped elements and/or transmission lines, or one could mechanically match the helical antenna with introducing metals strips to helical conductor. Examples of reducing the impedance by mechanical matching are to either place a triangular or a thin metal strip bounded to helical conductor near feed points, as illustrated in Figure 8.2 and Figure 8.3.

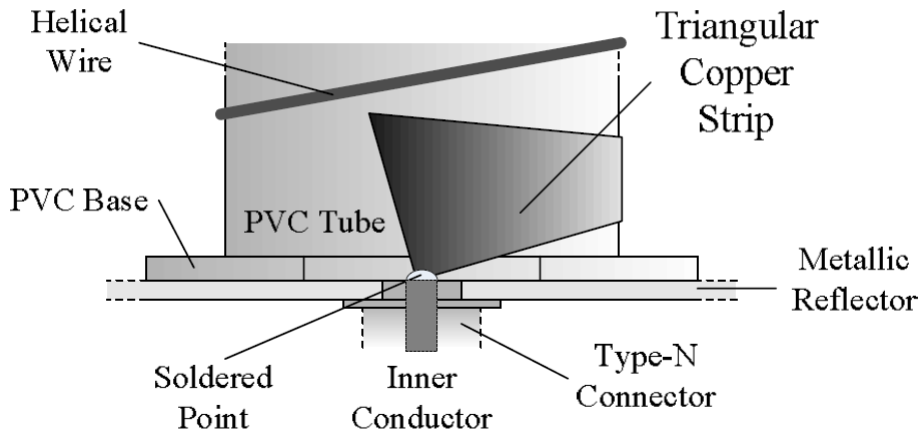


Figure 8.2: Impedance matching with triangular metal strip[35].

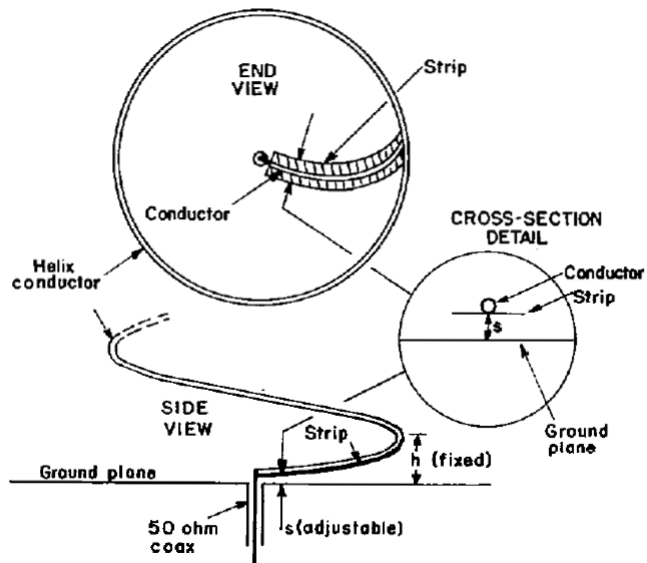


Figure 8.3: Impedance matching with a thin metal strip[36].

# Chapter 9

## Measurements and results

### 9.1 Instrumentation

For the antenna measurements the following was used:

- Echo free chamber, ca  $10\text{ m} \times 6\text{ m} \times 4\text{ m}$ , "reflection free" for  $f > 2\text{ GHz}$
- Antenna tower with a rotatable mounting disc
- Transmitting antenna, a double ridge horn, 1-15 GHz with a power amplifier HP 83020A
- Receiving reference antenna, a copy of the transmitting antenna
- Rotation controller, Newport MM4005
- Network analyzer HP 8720B for impedance measurements
- Network analyzer HP8510C for radiation pattern measurements
- 35 mm calibration kit HP 85052D
- Computers with the necessary MATLAB[34] programs and GP-IB interfaces

See Figure 9.1 for an overview of the echo free chamber with the instruments used for measuring.

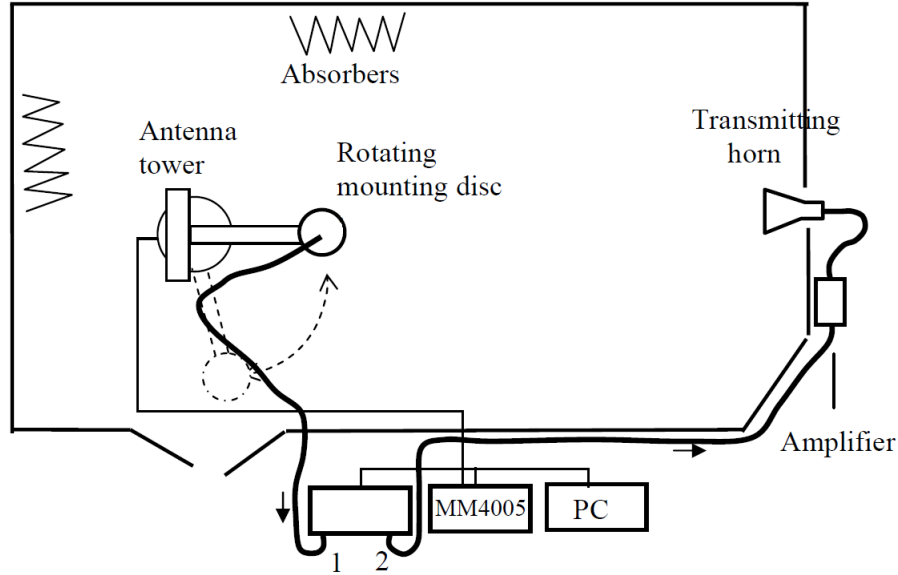


Figure 9.1: Echo free chamber with instruments for measuring[37].

## 9.2 Measurement explanations

Measurements of the antenna should be done in the far field, that is when  $r > 2D^2/\lambda$ . From Table 8.2 it is seen that  $D = 27.47$  cm and  $\lambda = 13.7$  cm, which gives far field for  $r > 87$  cm. The distance between the position of the transmitting antenna and the receiving test antenna is about 6 meters, so the far field criteria is fulfilled. Even though the measurements are done in the far field of the helical antenna, there will be a difference between the incident field and the field from a planar wave. This comes from the fact that the distance between the transmitting and receiving antenna is finite, and thus the spherical wave front is not exactly planar, and the maximum phase error of the incident field from an ideal planar wave is about  $22.5^\circ$ [25].

The gain can be calculated at least to different ways. First the gain can be calculated by comparing the measured field, in the direction of maximum gain, with the field of a reference antenna with known gain. The gain of the helical antenna is the gain of the reference antenna with the difference subtracted, however, to get the correct result, the mismatch losses must be included. Secondly, since the gain is inversely proportional with the square of the HPBW, the gain can be estimated by comparing a field with known gain, typically from a simulation, with a measured field. If the side lobes are approximately of the same size, then the difference in HPBW will show whether the gain is bigger, smaller or the same as the simulation.

From classic electromagnetism the reciprocity theorem gives that the characteristics of the antenna, like gain, field pattern, etc, are the same in transmitting and receiving mode. The measurements in the echo free chamber is done with the helical antenna in receiving mode since that is the most practical.

The transmitting horn antenna is placed in both horizontal and vertical position under the measurements, so that both polarizations are measured. Combined the polarizations represent the desired circular polarization.

## 9.3 Results

The measurement results are plotted in polar plots with direction in degrees on the circumference of the circle, and S12 in dB on radial axis. See Appendix D for the plots of the measurements with the different ground conductors. The gain are measured with two methods, the first is a comparison of HPBW and the second is a gain comparison between a reference antenna and the helical antenna.

### 9.3.1 Gain

In Table 9.1 a comparison is shown of the HPBW between measurements and simulation for the different ground conductors, for the center frequency 2.185 GHz. The values are taken from the plots in Figure D.1, D.7 and D.11. Since the field from the simulation is equal for the electric and magnetic field, as expected from circular polarization, only one of the fields is included in the table. Note that the plots are scaled in such manner that the direction with maximum gain is overlapping in the main beam, this is done so that it is possible to compare the results. The scaling is necessary even though the outline of the field should be similar for the simulation and the measurements. This comes as a consequence from the fact that the antenna is not impedance matched, the thus giving different size of the fields.

Ground conductor / HPBW	Horizontal	Vertical	Simulation
Flat	32.0°	32.0°	35.7°
Cupped	34.4°	34.4°	36.8°
Truncated cone	24.0°	26.8°	27.2°

Table 9.1: Comparison of the HPBW between the simulation and the measurements for the different ground conductors.

Additionally, measurements were done with two more frequencies, 2.175 GHz and 2.195 GHz, which are on each side of the center frequency 2.185 GHz. See Figure D.5 and D.6 for the plots for the flat ground conductor, Figure D.9 and D.10 for the plots for the cupped ground conductor and Figure D.13 and D.14 for the plots for the truncated cone ground conductor, for measurements with different frequency. There are two plots for each ground conductor since

there are done measurements with the transmitting horn in both horizontal and vertical position.

In Figure D.2, D.8 and D.12 are the measured field for each ground conductor compared with the the measured field for the reference horn antenna. The reference horn antenna is said to have 7.7 dB gain at 3 m for the frequency 2 GHz and is a copy of the transmitting horn. However, these are old data, and there have been years since the last calibration. Since the fasten mechanism was a little bit slack, the measurements were only done from about -90 to 90 degrees, which covers the significant area with the main beam. For the calculated return loss, difference in gain between the reference horn antenna and the helical antenna in the direction of maximum gain and the estimated total gain, see Table 9.2.

Ground conductor	Return loss	Difference in gain	Total gain
Flat	7.0 [dB]	1.4 [dB]	13.3 [dB]
Cupped	7.0 [dB]	1.5 [dB]	13.2 [dB]
Truncated cone	6.3 [dB]	0.9 [dB]	13.1 [dB]

Table 9.2: Reflection at the input port, return loss, difference in gain compared with reference horn antenna and the total gain for the different ground conductors.

Measurements were also done in another position in the echo free chamber, see Figure D.3 and D.4 for comparison of the field measured for the flat ground conductor in two different positions, measured with horizontal and vertical polarization. For a comparison of the different ground conductors in the same figure, see Figure D.15. At last the S11 for the antenna can be seen in the Smith chart in Figure D.16.

### 9.3.2 Impedance matching

The antenna reflects power at the input, as expected from the simulations, and the negative imaginary part implies that the impedance is capacitive. See Table 9.3 for a comparison between the simulated and measured reflection coefficients for the different ground conductors.

Ground conductor	Simulations		Measurements	
	S11	arg(S11)	S11	arg(S11)
Flat	5.2 [dB]	-74°	7.0 [dB]	-87°
Cupped	5.0 [dB]	-72°	7.0 [dB]	-92°
Truncated cone	4.7 [dB]	-73°	6.3 [dB]	-89°

Table 9.3: Comparison of the reflection coefficients from the simulation and the measurements.

From the table it is seen that the reflection coefficients are approximately

the same for the ground conductor variations. Note that no decimals are included since the S11 values had some fluctuations when they were read from the network analyzer. However, the measurements presents more reflection at the input than the simulations does. This could be due to that the simulations were done with perfect electric conductors with no loss. Nevertheless, the antenna must be impedance matched. This is done in Advanced Design System (ADS)[33]. A suggestion for matching network is an inductor in shunt and an inductor in series, which would convert the impedance to a real value of  $50 \Omega$ , see Figure D.16 and Figure D.17 in Appendix D.5.

## Chapter 10

# Discussion

The simulation at the center frequency showed that the maximum gains are 13.1 dB, 13.5 dB and 15.3 dB for the flat, the cupped and the truncated cone ground conductor, respectively. The simulated and measured HPBW almost coincides, in fact the measured gains are a little bit higher. This implicates that the simulation program is almost, but not fully able to imitate the real world. Still, this is an expected result, since the characteristics of an antenna are dependent on spatial variations with multipath propagation and interference. The measurements were done on a scale model, and a complete agreement between the simulations would be unrealistic, because some parameters, such as conductivity, are not scalable. Additionally, the simulations were done with perfect electric conductors and the measurements were done on lossy metals. The measuring method does not include losses introduced in the antenna, so even with a matching network, the total efficiency of the antenna is not accounted for.

The second method to measure the gain, i.e. comparing with a reference horn antenna, shows inconsistent results compared to the simulations. These measurements gave approximately 13 dB gain for all of the three ground conductors as seen in 9.2. This could partly be explained with the unmeasured conduction and dielectric losses introduced in the antenna. On the other hand this does not explain why there are almost no difference between the gains for the different ground conductors.

If the results from the first measure method are used, then the number of elements in the antenna array can be reduced from four to two, if the flat or the cupped ground conductor is chosen. The geometrical arrangement of a two-element array is only dependent of the distance between each element, so the optimum geometry can be found from simulating various distances between the elements. However, mutual coupling is also dependent of the amplitude current excitation, phase excitation and radiation pattern of each elements, so there are more factors than can be adjusted to achieve the highest total gain.

Both the flat and the cupped ground conductors present good polarization quality by having circular polarization in the main beam, as seen in Figure D.1 and Figure D.7. In the side lobes and back lobes however, the polarization is not

circular. This is in compliance with the use that is wanted from the antenna, since only the main beam is going to be used for communication.

The truncated cone ground conductor demonstrates a much higher gain than the two other ground conductors, and with some adjustments, 16 dB gain could be achieved with only one element in the array. On the other hand, the truncated cone ground conductor has significantly larger physical size, and this easier design might not compensate for the large physical size it introduces. In addition, the truncated cone ground conductor did not show as good circular polarization quality over the whole main beam as the two other ground conductors. Still the difference is not that big, as seen in Figure D.11.

The frequencies at 10 MHz lower and higher than the center frequency, show almost the same field pattern as the center frequency, for both horizontal and vertical polarization for all the three ground conductors. The Doppler shift for 437 MHz is about 11 kHz depending on the orbital height of the satellite. For the antenna at the ground station, this means that the bandwidth of the antenna should cover 435 - 439 MHz  $\pm$ 11 kHz. The measured field pattern for the antenna at different frequencies gives an indication that the antenna has linear gain characteristics around the center frequency.

To achieve an insight of the effects of the room reflections on the irregular side lobes, additional measurements were done at another location in the echo free chamber, for the case with the flat ground conductor. The rotated and scaled fields are seen in Figure D.3 and Figure D.4. They present unequal field patterns, especially for the side and back lobes for both horizontal and vertical polarization. This implies that the echo free chamber is not perfect, which can be explained with the reflections from the door, and the small path without absorbers between the door and the antenna tower.

The reflection coefficient measured at the input of the antenna showed that an impedance matching will be necessary to achieve better efficiency. A suggestion for the impedance matching was carried out for the flat ground conductor, however other matching networks are also possible.

# Chapter 11

## Conclusion

The presented antenna design is a feasible solution for the ground station antenna for UHF. The measurements on the model were in accordance with the simulations, which shows that optimizations can be done in the simulation software.

The link budget stated that 16 dB gain in the ground station antenna would suffice, and the measurements showed that this is possible to achieve with only two elements in the antenna array if the flat or the cupped ground conductor is used. Furthermore, if the truncated cone ground conductor is used and some adjustments are done, 16 dB gain will be achievable with only one element in the array. In contrast, this would give a much bigger wind load, and since several shorter elements in an array are preferred over a single long element, it is suggested that an array with two elements is used. Still there are some losses that are not accounted for, so less gain than stated in the first gain measuring method is expected. Moreover, it is suggested that the ground conductor is made with perforation to decrease the wind load.

The full scale antenna array will be compatible with the radio transceiver at the ground station, and a better result will be achieved with impedance matching. Additionally, since the operative antenna rig is mounted, a change between the UHF Yagi Uda and this helical antenna design will make the helical antenna steerable in the desired elevation and azimuth degrees.

### 11.1 Future work

If this work is continued, there is some work left before the helical antenna design is ready. This includes:

- Optimize the design in the simulation software
- Choose a ground conductor. The flat or the cupped ground conductor with perforation is recommended
- Determine the supporting structure inside the helical antennas

- Decide the distance between the two elements in the antenna array
- Construct the antenna array in correct scale
- Impedance match the antenna structure to  $50 \Omega$

# Bibliography

- [1] Mireia Oliver Miranda. Design of ground station antenna for a double CubeSat student project, 2007.
- [2] Laurea Magistrale. Design and Realization of a Ground Station Antenna for a Small Student Satellite, 2008.
- [3] Beathe Hagen Stenhaug. Feasibility Study of a Ground Station for NTNU Test Satellite, 2011.
- [4] Timothy Pratt, Charles Bostian and Jeremy Allnut. *Satellite Communications, second edition*. John Wiley & Sons, 2003. ISBN: 0-471-37007-X.
- [5] Anil K. Maini and Varsha Agrawal. *Satellite Technology, second edition*. John Wiley & Sons, 2011. Online ISBN: 978-0-470-71173-6.
- [6] SP 7000 low noise mast-mounted GaAsFET preamplifier from SSB Electronic. URL: <http://www.ssb.de/>
- [7] SGL 0622Z low noise MMIC amplifier silicon germanium from RF Micro Devices. URL: <http://www.rfmd.com/>
- [8] Specification for Icom IC-9100 from Icom America Inc. URL: <http://www.icomamerica.com/en/products/amateur/hf/9100/specifications.aspx>.
- [9] Jan King's link budget spreadsheet, from AMSAT-IARU. URL: <http://www.amsat.org.uk/iaru/>
- [10] Louis J. Ippolito Jr. *Satellite Communications System Engineering*. John Wiley & Sons, 2008. ISBN: 978-0-470-72527-6.
- [11] Roger Birkeland, Elisabeth Blom and Erik Narverud. Design of a Small Student Satellite, 2006.
- [12] Map over Electro Block D at Gløshaugen Campus. URL: <http://www.ntnu.no/kart/kart-over-ntnu/gloeshaugen/elektro-d-b2/5-etasje/>

- [13] GENSO. URL: <http://www.genso.org/>
- [14] Dharma Raj Cheruku. *Satellite Communication*. I.K. International Publishing House Pvt. Ltd., 2009. ISBN: 978-93-80026-41-1.
- [15] WXtrack by David J Taylor, Edinburgh, URL:<http://www.satsignal.eu/software/wxtrack.htm>.
- [16] John D. Holmes. *Wind Loading of Structures*. Spoon Press 2001. ISBN: 978-0-419-24610-7.
- [17] David K. Cheng. *Field and Wave Electromagnetics*. Addison - Wesley, 1989. ISBN 0-201-52820-7.
- [18] Kenneth G. Budinski and Michael K. Budinski. *Engineering Materials, seventh edition*. Pearson Education, Inc. 2002. ISBN: 0-13-030533-2.
- [19] Hisamatsu Nakano, Junji Yamauchi, Hiroaki Mimaki. *Backfire Radiation from a Monofilar Helix with a Small Ground Plane*. IEEE Transactions of antennas and propagation, vol. 36, no 10, October 1988.
- [20] Antonije R. Djordjević, Alenka G. Zajić, Milan M. Ilić. *Enhancing the Gain of Helical Antennas by Shaping the Ground Conductor*. IEEE Antennas and wireless propagation letters, vol. 5, 2006.
- [21] H.T. Hui, Edward K.N. Yung, C.L. Law, Y.S. Koh and W.L. Koh. *Design of a Small and Low-Profile 2x2 Hemispherical Helical Antenna Array for Mobile Satellite Communications*. IEEE Transactions on Antennas and propagation, vol. 32, no. 1, January 2004.
- [22] H.T. Hui, K.Y. Chan and E.K.N. Yung. *The Input Impedance and the Antenna Gain of the Spherical Helical Antenna*. IEEE Transactions on Antennas and Propagation, vol. 49, no 8, August 2001.
- [23] David M. Pozar. *Microwave and RF design of wireless systems*. John Wiley & Sons, 2001. ISBN: 0-471-32282-2.
- [24] Constantine A. Balanis. *Antenna Theory - Analysis and Design*. John Wiley & Sons, 2005. ISBN 0-471-66782-X.
- [25] Constantine A. Balanis. *Modern Antenna Handbook*. John Wiley & Sons, 2008. ISBN: 978-0-470-03634-1.
- [26] Thomas A. Milligan. *Modern Antenna Design, second edition*. John Wiley & Sons, 2005. ISBN: 978-0-471-45776-3.
- [27] Peter Berlin. *Satellite Platform Design*. Department of Space Science of the Universities of Luleå and Umeå, 2005. ISBN: 978-91-633-0324-1.

- [28] Andøya Rocket Range. URL: <http://www.rocketrange.no/>
- [29] Antonije R. Djordjević, Alenka G. Zajić, Milan M. Ilić and Gordon L. Stüber. *Optimization of Helical Antennas*. IEEE Antennas and Propagation Magazine, vol. 48, no. 6, pp. 107-116, December 2006.
- [30] CST MICROWAVE STUDIO® from  
CST STUDIO SUITE™2010. URL:  
<http://www.cst.com/Content/Products/MWS/Overview.aspx>
- [31] EMpro 3D Simulation Software from Agilent Technologies. URL:  
<http://www.home.agilent.com/agilent/home.jsp?cc=NO&lc=eng>
- [32] Divinycell H100. Data sheet, URL:  
<http://www.matweb.com/search/datasheettext.aspx?matid=29807>
- [33] Advanced Design System from Agilent Technologies. URL:  
<http://www.home.agilent.com/agilent/home.jsp?cc=NO&lc=eng>
- [34] MATLAB - for technical computing. URL:  
<http://www.mathworks.com/products/matlab/>
- [35] V. Wongpaibool. Improved Axial-Mode-Helical-Antenna Impedance Matching Utilizing Triangular Copper Strip for 2.4-GHz WLAN URL:  
[http://ieeexplore.ieee.org/xpls/abs\\_all.jsp?arnumber=4600049](http://ieeexplore.ieee.org/xpls/abs_all.jsp?arnumber=4600049)
- [36] John D. Kraus. A 50-ohm Input Impedance for Helical Beam Antennas. URL:  
[http://ieeexplore.ieee.org/xpls/abs\\_all.jsp?arnumber=1141687](http://ieeexplore.ieee.org/xpls/abs_all.jsp?arnumber=1141687)
- [37] TTT4215 Antenna Techniques. Antenna Lab Instructions, Spring 2010. Author Unknown.
- [38] IEEE Standard Definitions of Terms for Antennas, IEEE Std 145-1993. URL:  
[http://ieeexplore.ieee.org/xpls/abs\\_all.jsp?arnumber=286098&tag=1](http://ieeexplore.ieee.org/xpls/abs_all.jsp?arnumber=286098&tag=1).
- [39] John D. Kraus, Ronald J. Marhefka. *Antennas For All Applications, third edition*. McGraw-Hill Companies, Inc., 2002. ISBN: 0-07-112240-0.
- [40] Dr D.T Emerson. The Gain of the Axial-Mode Helix Antenna. Antenna Compendium Volume 4, pp.64-68, 1995. URL:  
<http://www.tuc.nrao.edu/~demerson/helixgain/helix.htm>

Part III

Appendices

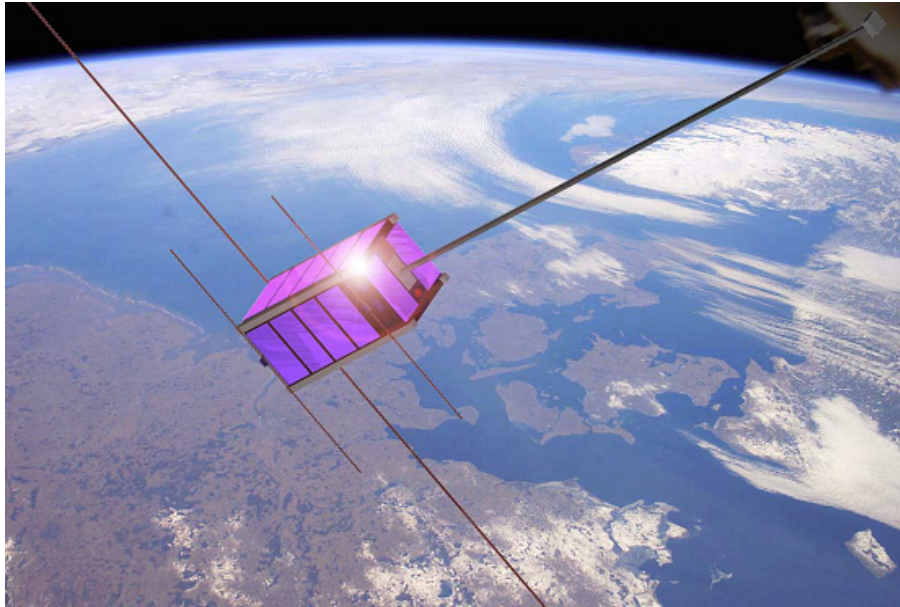
## Appendix A

# NUTS-1 Mission Statement

# NUTS-1 Mission Statement

Roger Birkeland

June 14, 2011



## 1 Background

The NUTS (NTNU Test Satellite) project was started in September 2010. The project is part of the Norwegian student satellite program run by NAROM (Norwegian Centre for Space-related Education) [1]. The projects goal is to design, manufacture and launch a double CubeSat by 2014. The national student satellite program involves three educational establishments, namely the University of Oslo (UiO), Narvik University College (HiN) and NTNU.

### 1.1 Mission Statement

The NUTS project aims to design, develop, test, launch and operate a double CubeSat by 2014. Students from different curiums will do the largest part of the work, supported by project management and technical staff. The work will be performed as part of the students project- and master theses. We have chosen our design to be generic and modular, so the satellite-bus can support different pay loads. As payload for the first satellite, an IR-camera will be implemented, in addition to a wireless internal databus.

Recruitment and education of skillful students will be a main part of the projects goals. Through hands-on experience, the students will be able to master different skills needed in their jobs after graduation.

### 1.2 Mission Goals

- Deliver a tested satellite according to mission specifications
- Transmit a beacon signal receivable for radio amateurs
- Confirm successful de-tumbling
- Establish two-way communication and receive full telemetry
- Test IR camera
- Test RF intra-satellite bus
- Initiate camera pointing
- Initiate IR camera sequence
- Receive a valid series of images

The list above shows the tentative mission goals as of June 2010. As the project evolves, the mission goals may be changed and adapted. One other main goal, not mentioned above, is to educate students. This goal will be met even if none of the goals above are fulfilled.

## 2 About NUTS

Our satellite will be a double CubeSat, complying to the CubeSat Specification [3]. However, our satellites electronics will not be build around the "standard" PC-104 form factor. Instead, have chosen to use a design with a backplane. See Figure 1. This concept was first planned in 2006 [2]. Through this backplane, the different sub systems will access the main I<sup>2</sup>C communications bus as well as the power buses.



**Figure 1:** A 3D-model of NUTS-1

Use of other materials for the satellite structure will also be investigated.

### 2.1 Bus Concept

Our bus concept differs from many CubeSats since we do not use the PC-104 form factor for our electronics cards. There are several reasons for this: We want to try something new, we want to enhance the power and data buses and we feel that the backplane strategy provides us with an easier setup in the development and testing phase. The main draw back is that this leaves us quite "alone" since we now have heavily reduced our possibility to buy COTS modules for our satellite.

Our goal is that our bus concept can be used for a broad variety of payloads. For the first satellite, we have chosen to look into the use of a IR camera to observe the Earths atmosphere as well as an internal RF communication link. The on-board OBC is a powerful 32-bit AVR32 UC3

micro controller with a lot of computing capacity to support payloads in other missions as well.

To enhance the reliability of the satellite, we have decided to have to backplane masters in the satellite. This means that both the OBC and the communication system are able to remove other subsystems from the backplane power- and data buses. The communication system can be controlled directly from ground, but these capabilities should not be used unless the OBC has failed.

## 2.2 Payload

As main payload, the NUTS project will fly an IR-camera for atmospheric observations. In addition, a concept for a wireless short range data bus connecting different subsystems will be added. For communication, the satellite will use the common amateur radio bands and fly one transceiver for each frequency.

## 2.3 Ground station

In conjunction with our lab, we have set up a ground station for use with our satellite. Figure 2 shows pictures of our equipment.

Ground station equipment:

- 5 meter antenna mast
- Tonna 2x9 crossed Yagi-Uda for VHF
- Tonna 2x19 crossed Yagi-Uda for UHF
- Yaesu 5500 antennae rotor
- ICom IC-9100 radio
- ICom PCR-1500 radio for weather data download



**Figure 2:** Our ground station antenna mast to the left and our ground station radio and PC at the right

### 3 Education

The project is highly multidisciplinary. We need project members, both students and staff, from various departments. As examples, IET (Department of Electronics and Telecommunication), ITK (Department of Engineering Cybernetics), IPM (Department of Engineering Design and Materials), PHYS (Department of Physics), IDI (Department of Computer and Information Science) and ITEM (Department of Telematics) can be listed. The project is run and managed by IET, but students for the different departments must be supported and have a guidance teacher at their home department.

The satellite lab and ground station room serves as a common place for project members to study and work together. The use of this lab is vital for the project. However, each student should have access to a private and quiet work space also.

During the first half of 2011, ten students from different departments and curriculums were involved in the project.

Since we are developing our own bus concept, we cannot buy COTS subsystems, we are on our own in this matter. However, we believe that NTNU as a broad education provider should have enough resources and specialist environments to cover the whole spectrum of knowledge and skills needed.

#### 3.1 PR and Outreach

The project will use Internet for public outreach, as well as other printed media. Our web page is <http://nuts.iet.ntnu.no>. In addition, we are on Twitter (@NUTS\_Sat) and on Facebook. These pages and profiles will be frequently updated as the project moves forward.

### 3.2 Conferences

NUTS will be presented at SmallSat 2011, as a part of the University Exhibits. Two students will present their theses work at IAC in October this year also.

### References

- [1] NAROM. Narom home page, 2011. URL <http://www.narom.no>. Online.
- [2] Erik Narverud Roger Birkeland, Elisabeth Karin Blom. Design of a small student satellite. Project work, NTNU, 2006.
- [3] Cal Poly SLO The CubeSat Program. Cube-sat design specification rev. 12, 2011. URL [http://www.cubesat.org/images/developers/cds\\_rev12.pdf](http://www.cubesat.org/images/developers/cds_rev12.pdf). Online.

# Appendix B

## Simulation results

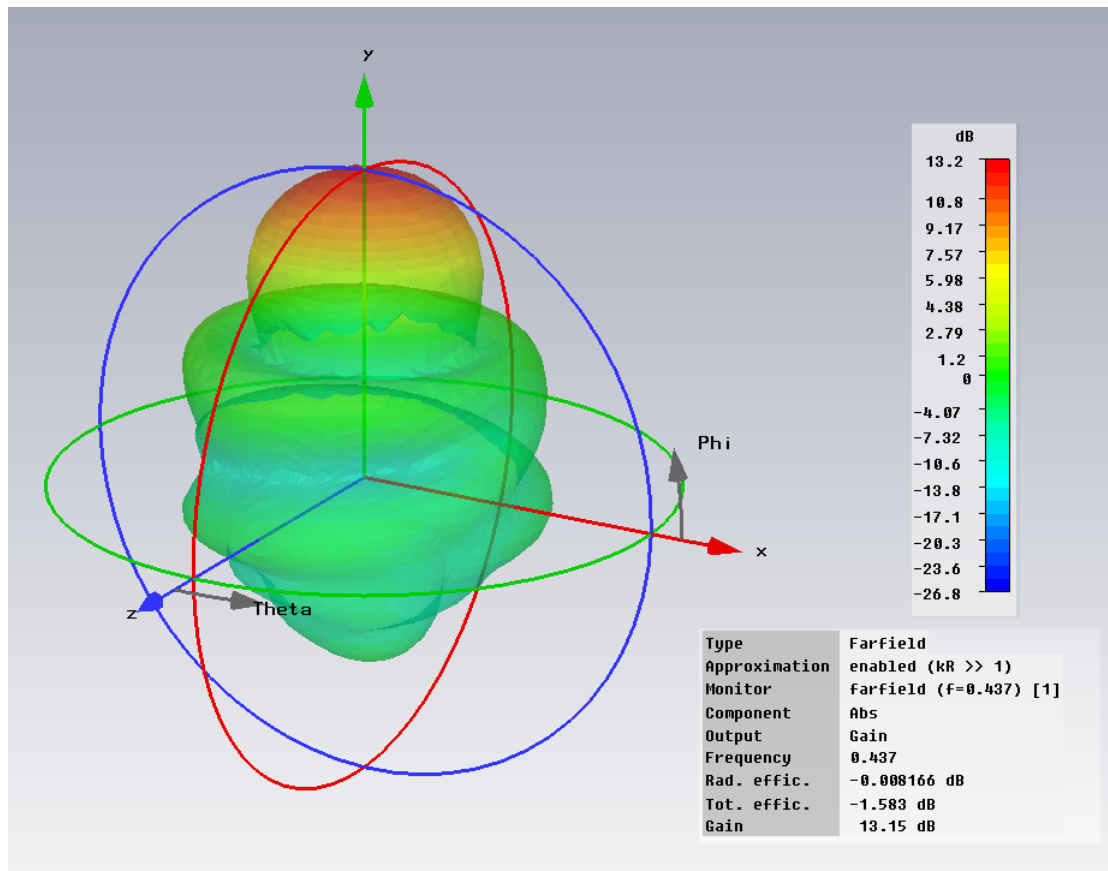


Figure B.1: The absolute gain in 3D for the flat ground conductor at 437 MHz.

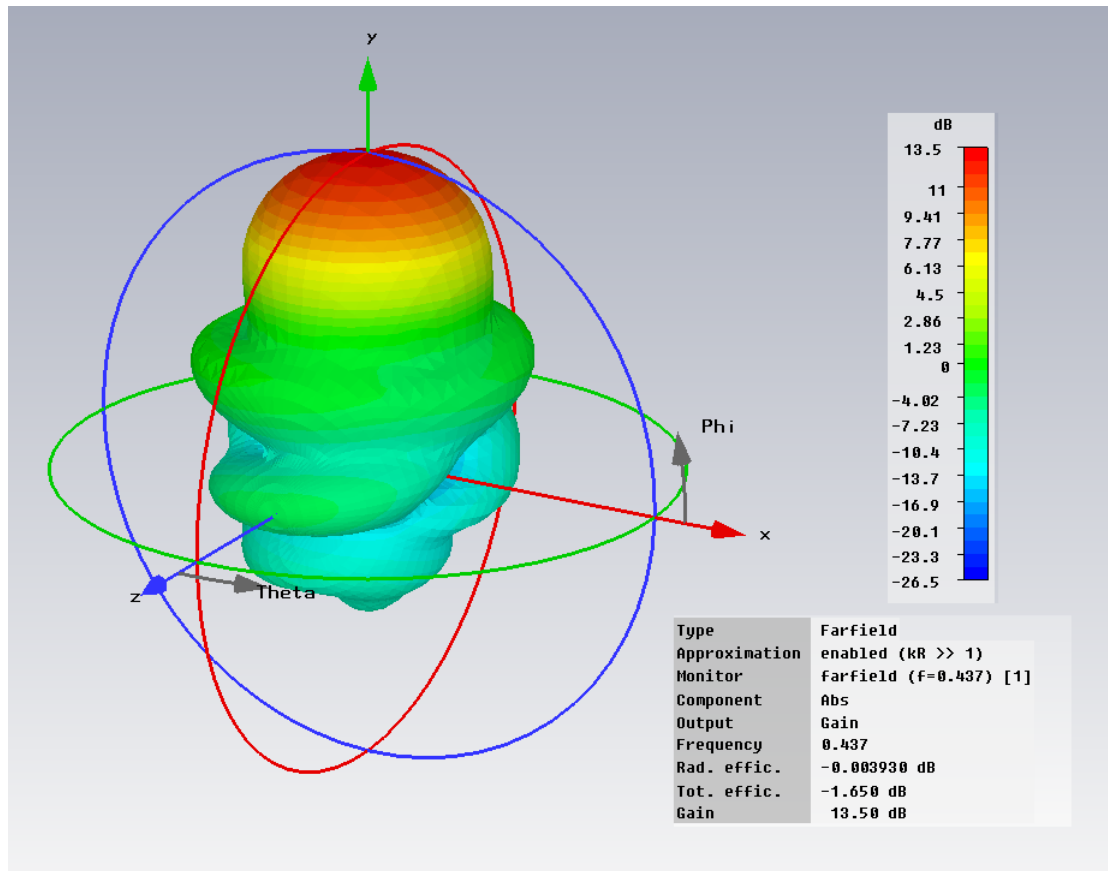


Figure B.2: The absolute gain in 3D for the cupped ground conductor at 437 MHz.

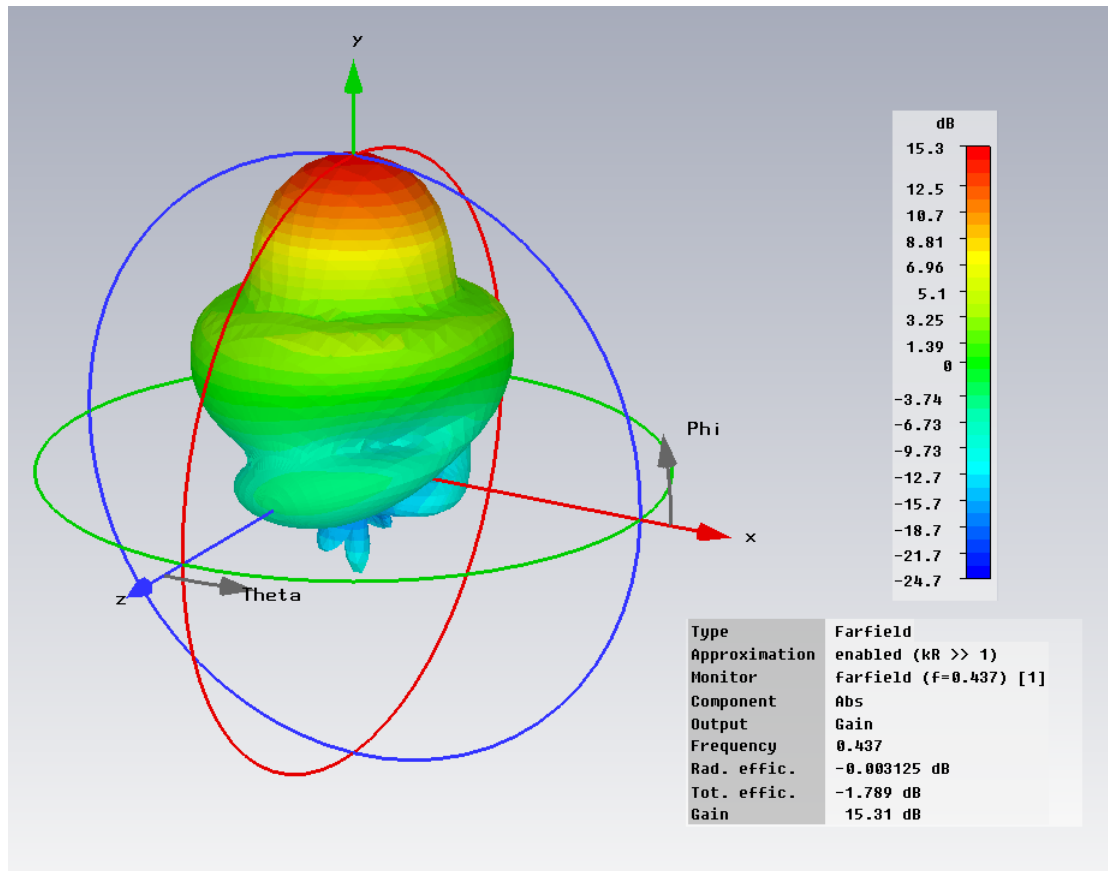


Figure B.3: The absolute gain in 3D for the truncated cone ground conductor at 437 MHz.

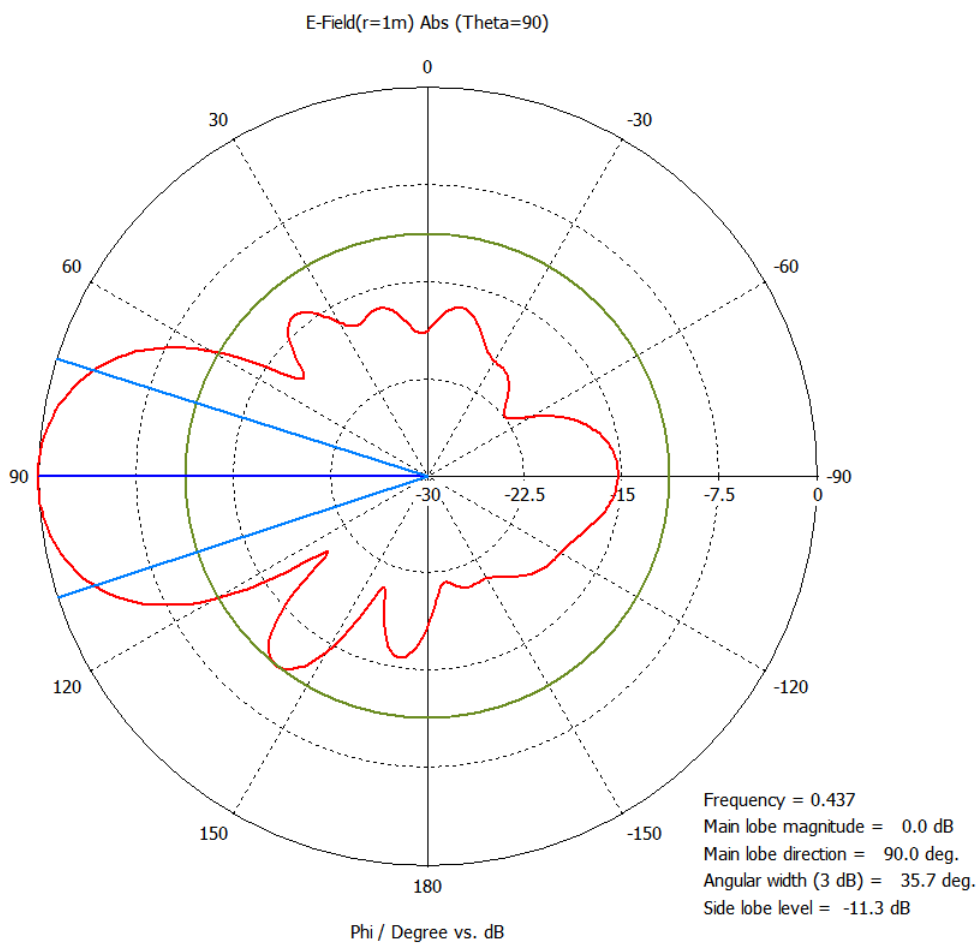


Figure B.4: E-field for the flat ground conductor at the frequency 437 MHz.

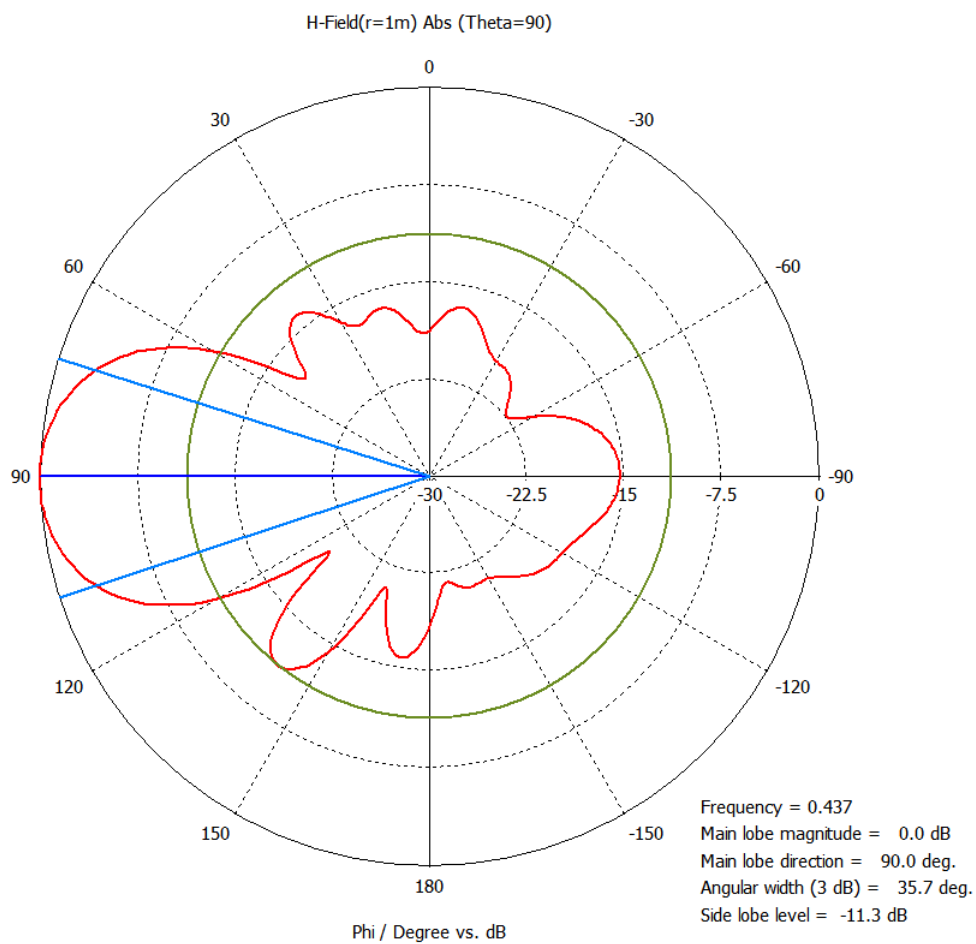


Figure B.5: H-field for the flat ground conductor at the frequency 437 MHz.

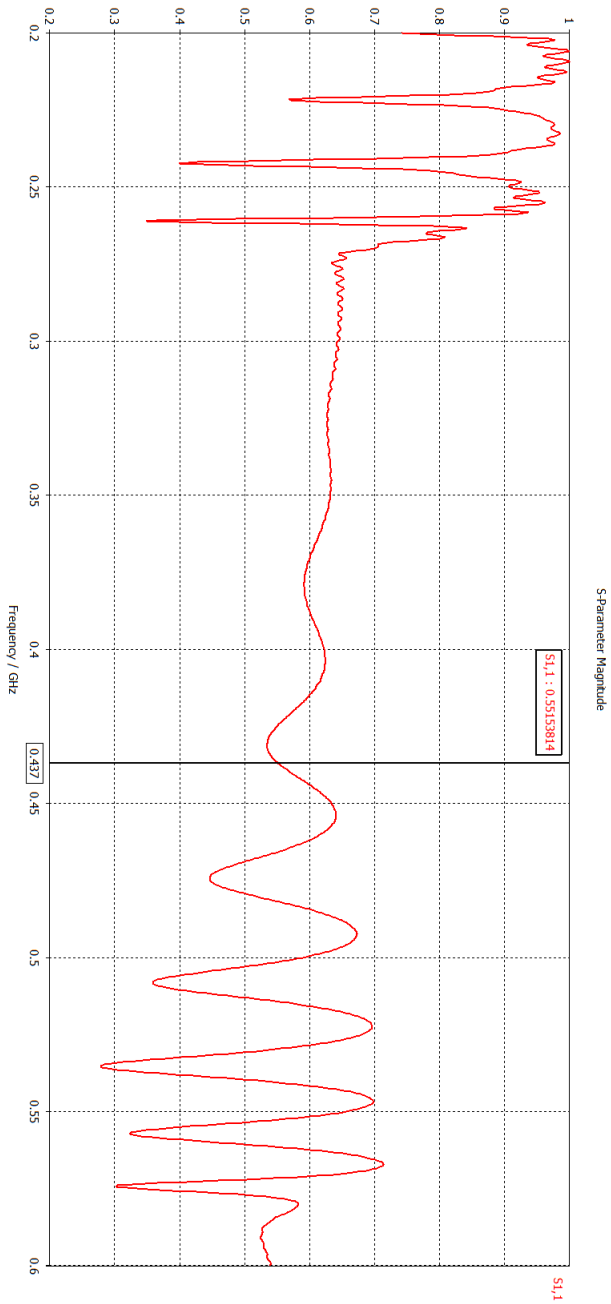


Figure B.6: The linear magnitude of S11 for the flat ground conductor at the frequency range 200 - 600 MHz.

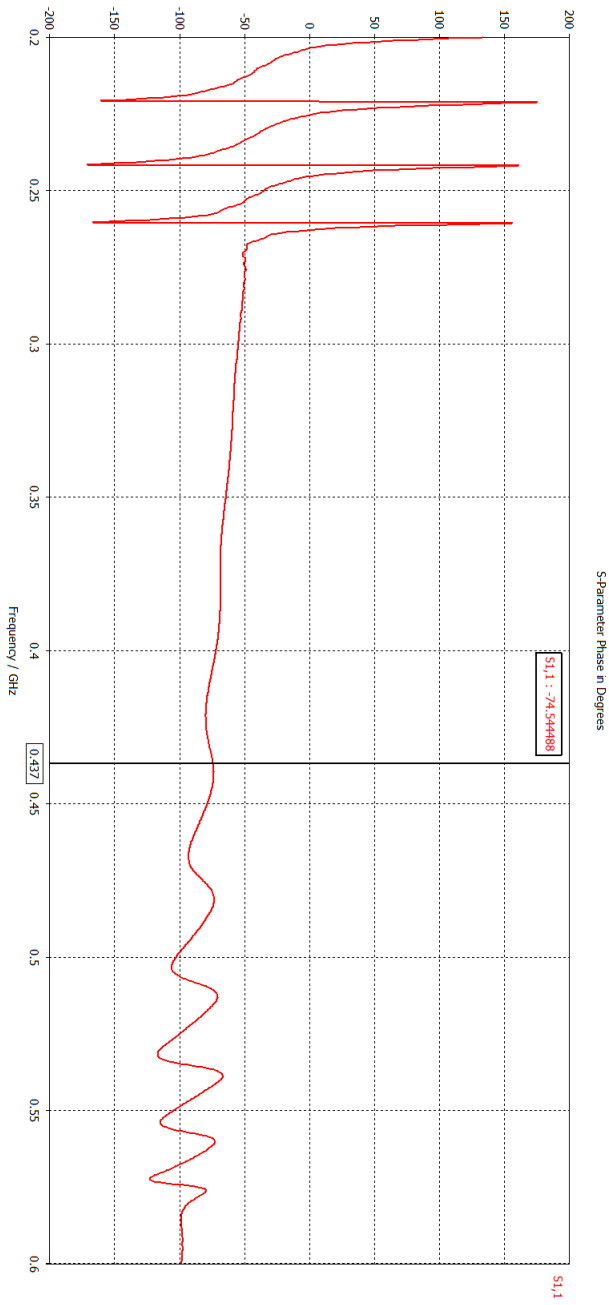


Figure B.7: The phase of S11 for the flat ground conductor at the frequency range 200 - 600 MHz.

## Appendix C

# The helical antenna model with ground conductors



Figure C.1: The helical antenna with the cupped ground conductor. On the right side of the figure is the 90 degree corner angle bracket in plastic for mounting the antenna on the rotating disc.



Figure C.2: The connection point between the copper wire and the feed point. The feed is a  $50\ \Omega$  type N connector.



Figure C.3: The back side of one of the ground conductors. In the upper part of the figure is the connector and in the lower part of the figure is the bracket for fastening the antenna on the rotating disc.



Figure C.4: The flat ground conductor.



Figure C.5: The cupped ground conductor.



Figure C.6: The truncated cone ground conductor. Top: side view. Bottom: top view.



Figure C.7: Comparison of the different ground conductor sizes.

## Appendix D

### Measuring results

## D.1 Measurements with the flat ground conductor

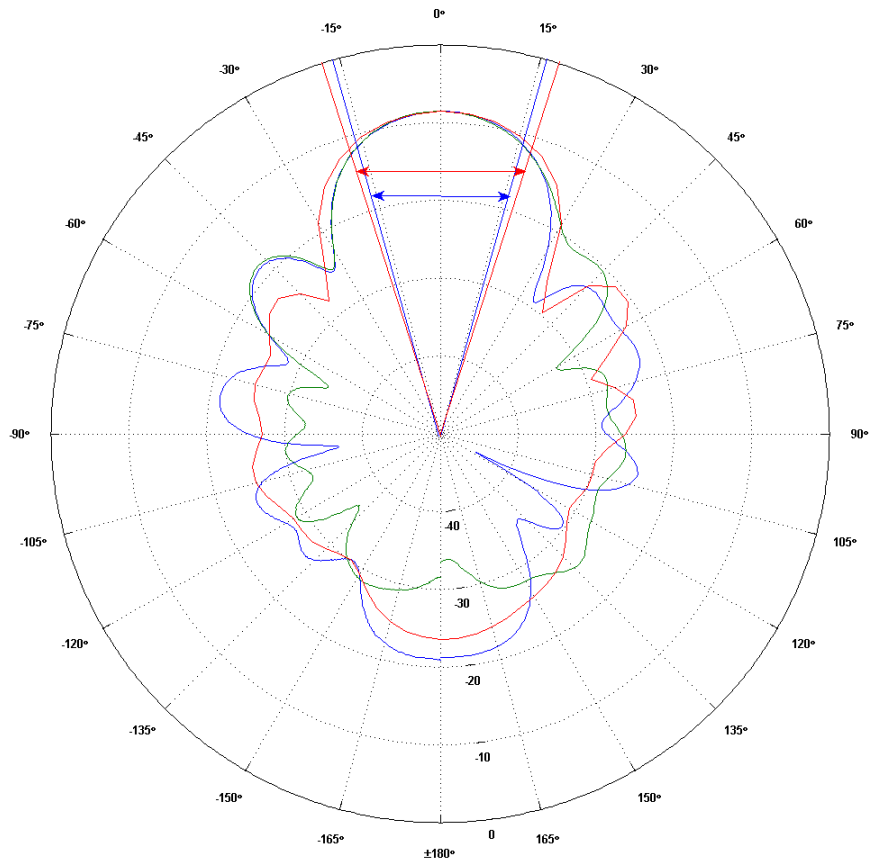


Figure D.1: The field pattern with half power beam width for the helical antenna measured for 2.185 GHz. The blue and green plots are for the transmitting horn antenna in horizontal and vertical position. The red plot is results from the simulation.

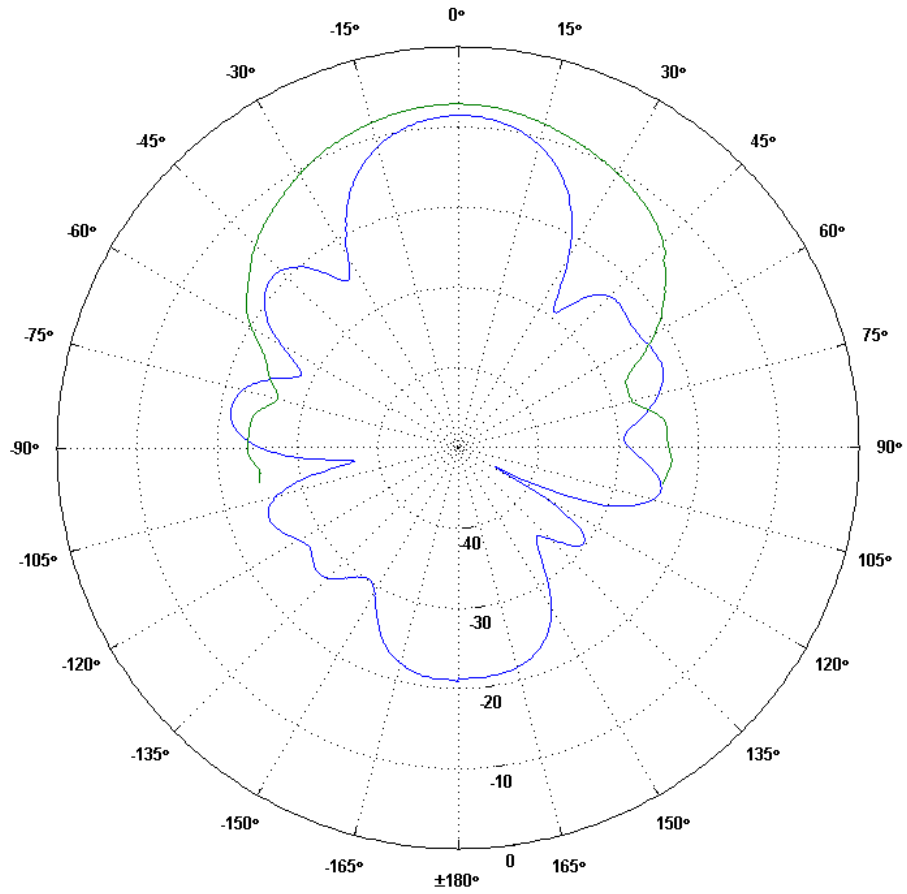


Figure D.2: The field pattern measured for the helical antenna marked blue compared with the field pattern for the reference horn antenna marked green.

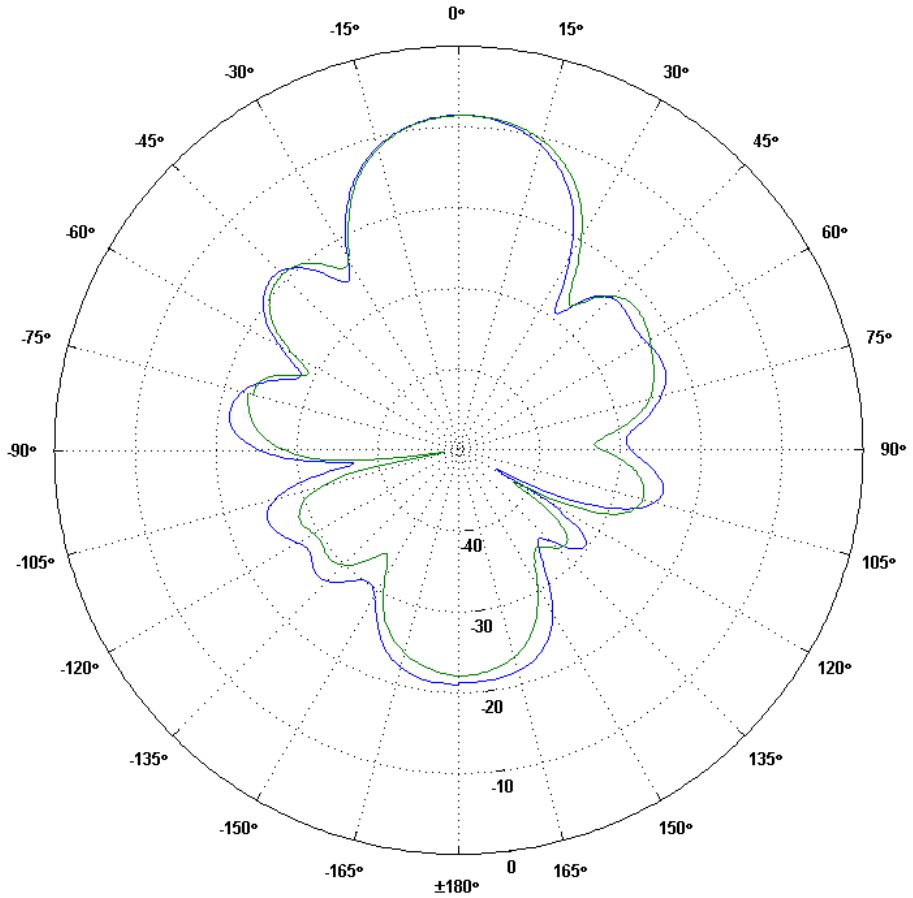


Figure D.3: The horizontal field pattern measured at two different positions in the echo free chamber. The blue plot are measurements at original position and the green plot are measurements from a new position, approximately two meter further away from the transmitting horn antenna.

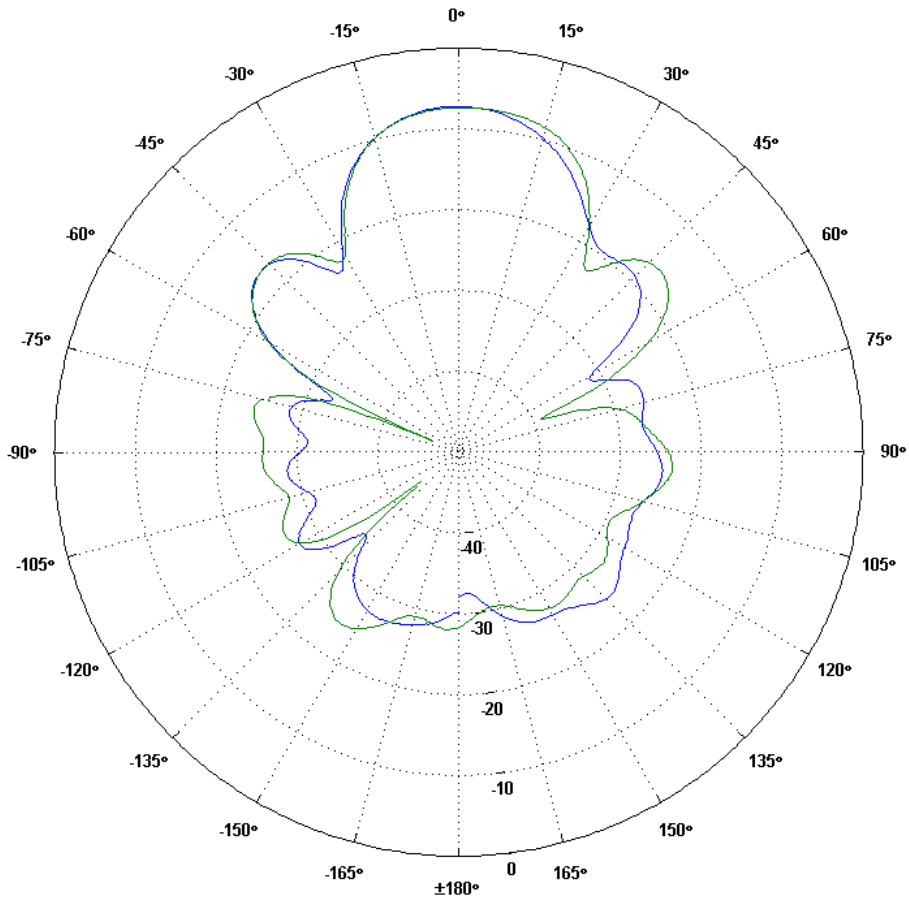


Figure D.4: The vertical field pattern measured at two different positions in the echo free chamber. The blue plot are measurements at original position and the green plot are measurements from a new position, approximately two meter further away from the transmitting horn antenna.

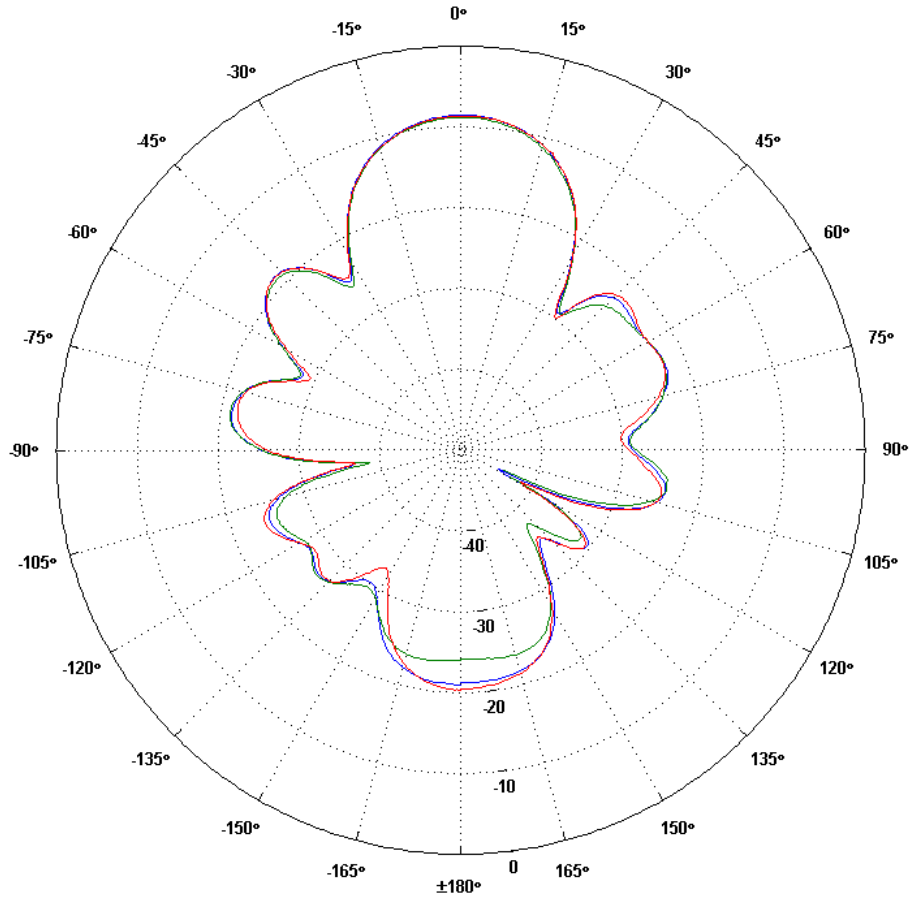


Figure D.5: Comparison of the field pattern for different frequencies. 2.175 GHz is marked blue, 2.185 GHz is marked green and 2.195 GHz is marked red. Measurements are done with horizontal polarization of the transmitting horn antenna.

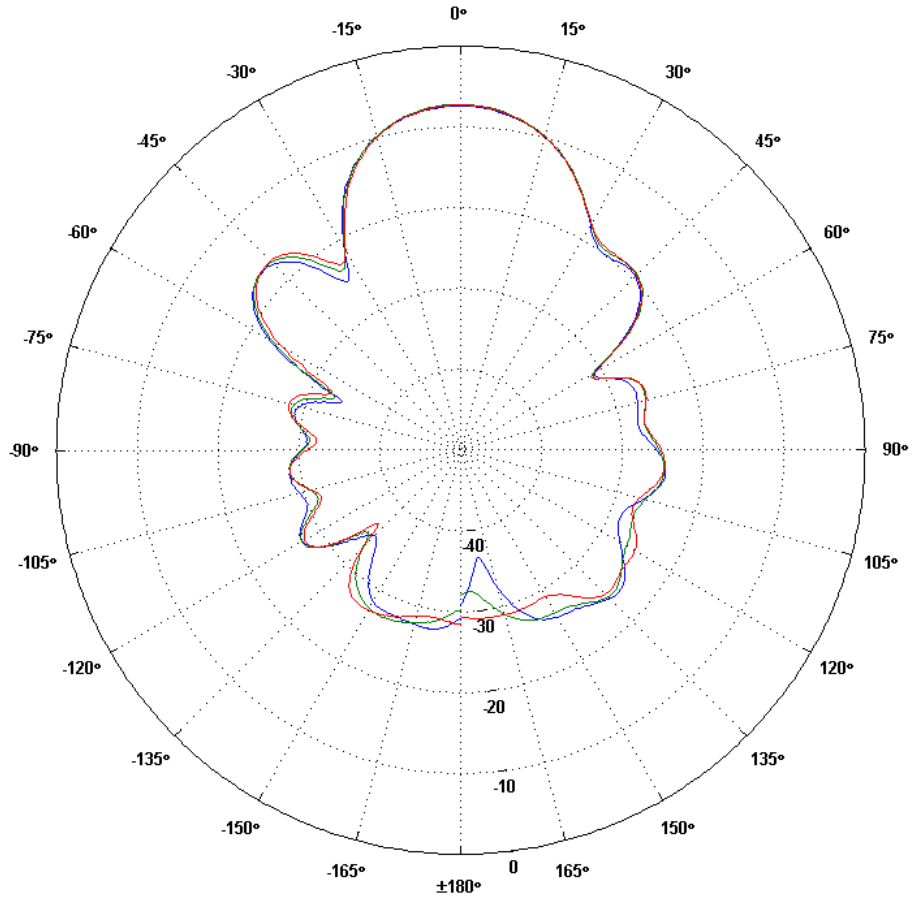


Figure D.6: Comparison of the field pattern for different frequencies. 2.175 GHz is marked blue, 2.185 GHz is marked green and 2.195 GHz is marked red. Measurements are done with vertical polarization of the transmitting horn antenna.

## D.2 Measurements with the cupped ground conductor

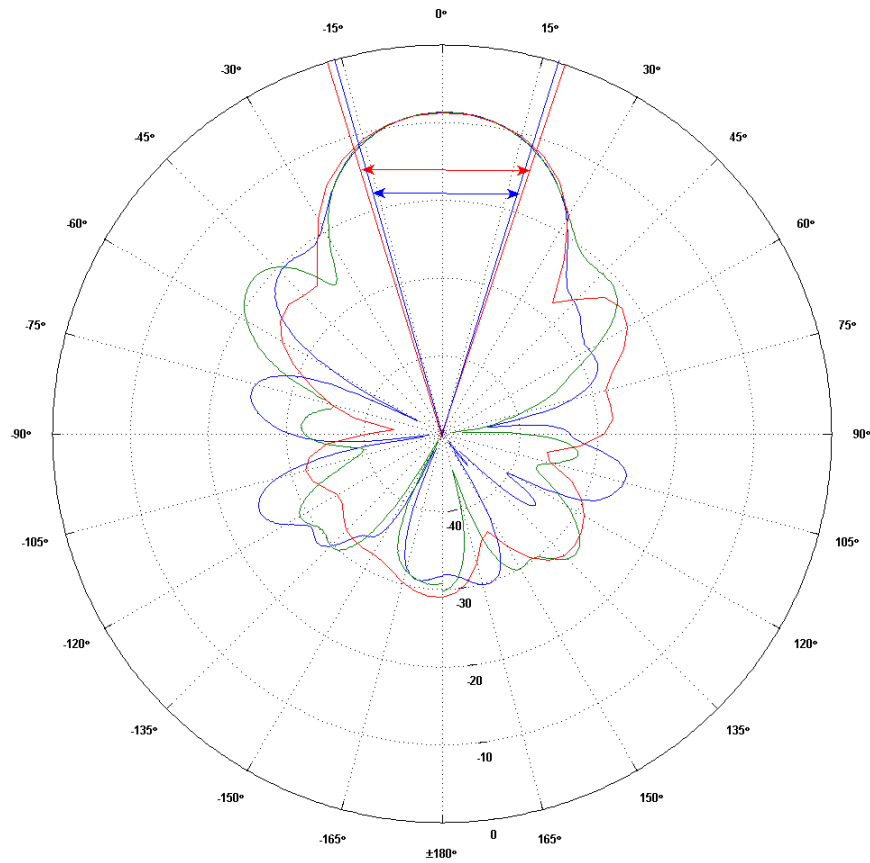


Figure D.7: The field pattern with half power beam width for the helical antenna measured for 2.185 GHz. The blue and green plots are for the transmitting horn antenna in horizontal and vertical position. The red plot is results from the simulation.

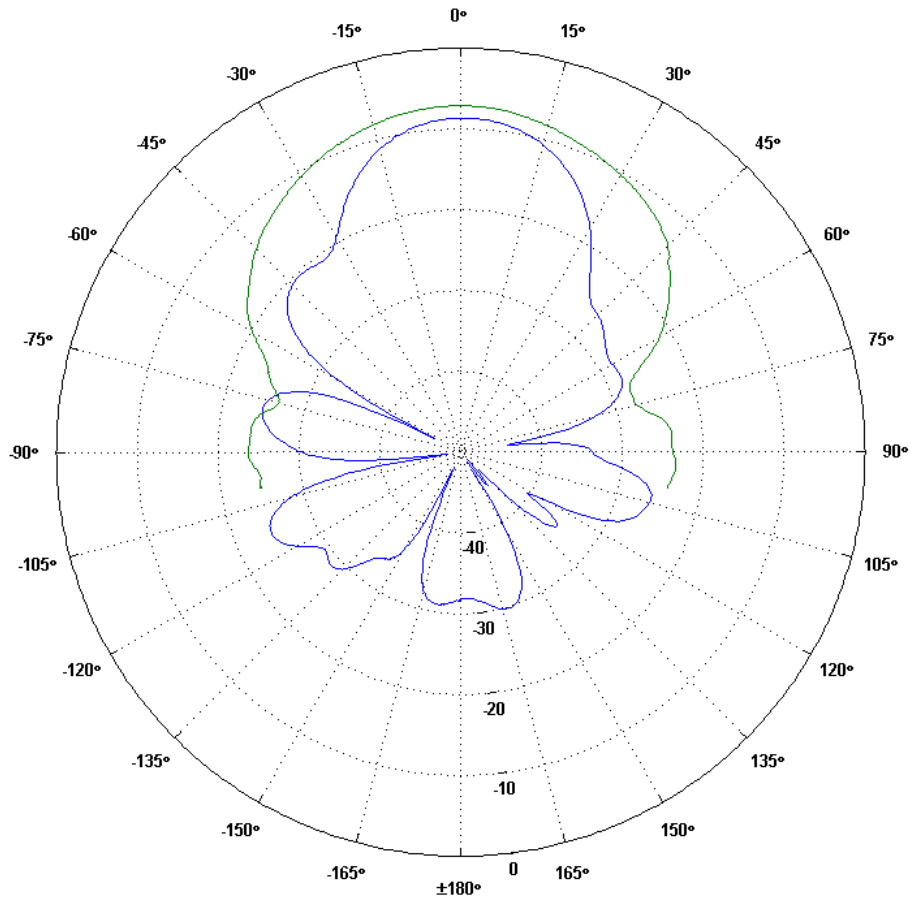


Figure D.8: The field pattern measured for the helical antenna marked blue compared with the field pattern for the reference horn antenna marked green.

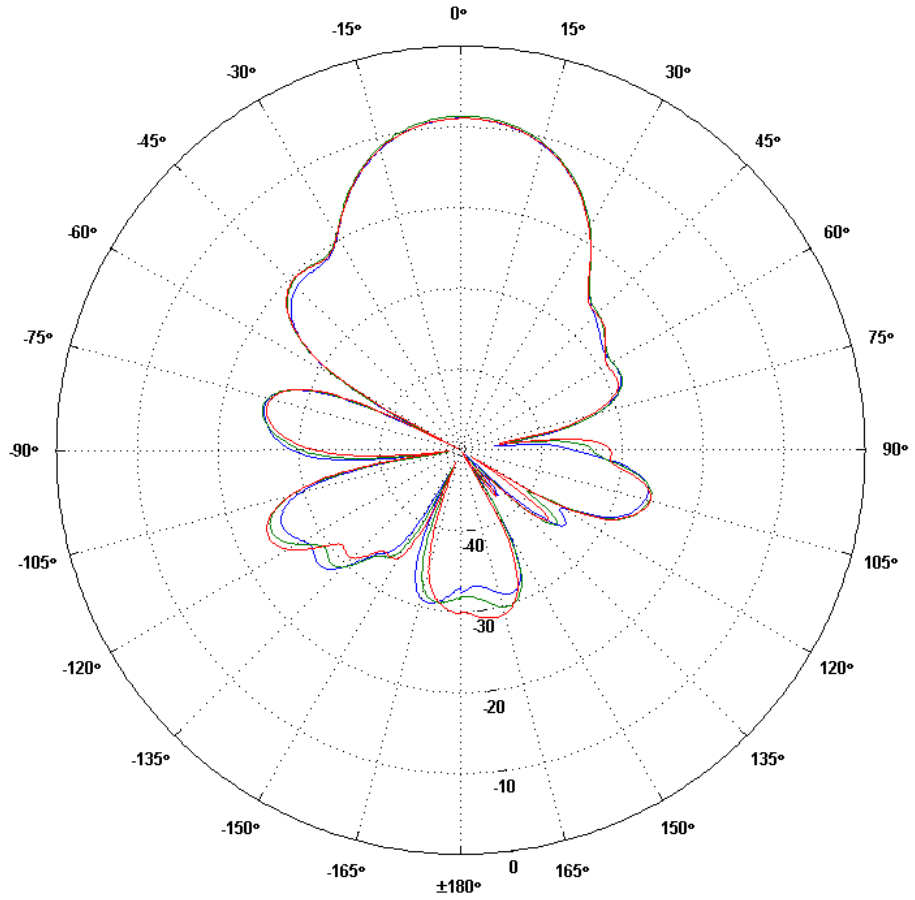


Figure D.9: Comparison of the field pattern for different frequencies. 2.175 GHz is marked blue, 2.185 GHz is marked green and 2.195 GHz is marked red. Measurements are done with horizontal polarization of the transmitting horn antenna.

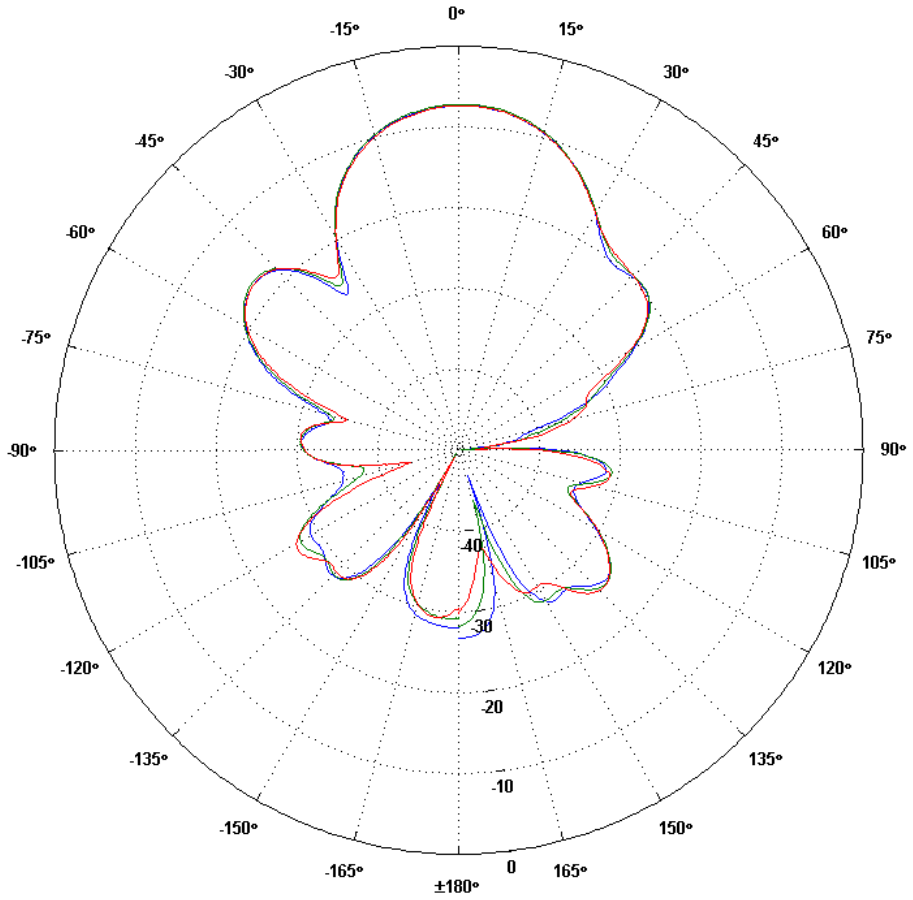


Figure D.10: Comparison of the field pattern for different frequencies. 2.175 GHz is marked blue, 2.185 GHz is marked green and 2.195 GHz is marked red. Measurements are done with vertical polarization of the transmitting horn antenna.

### D.3 Measurements with the truncated cone ground conductor

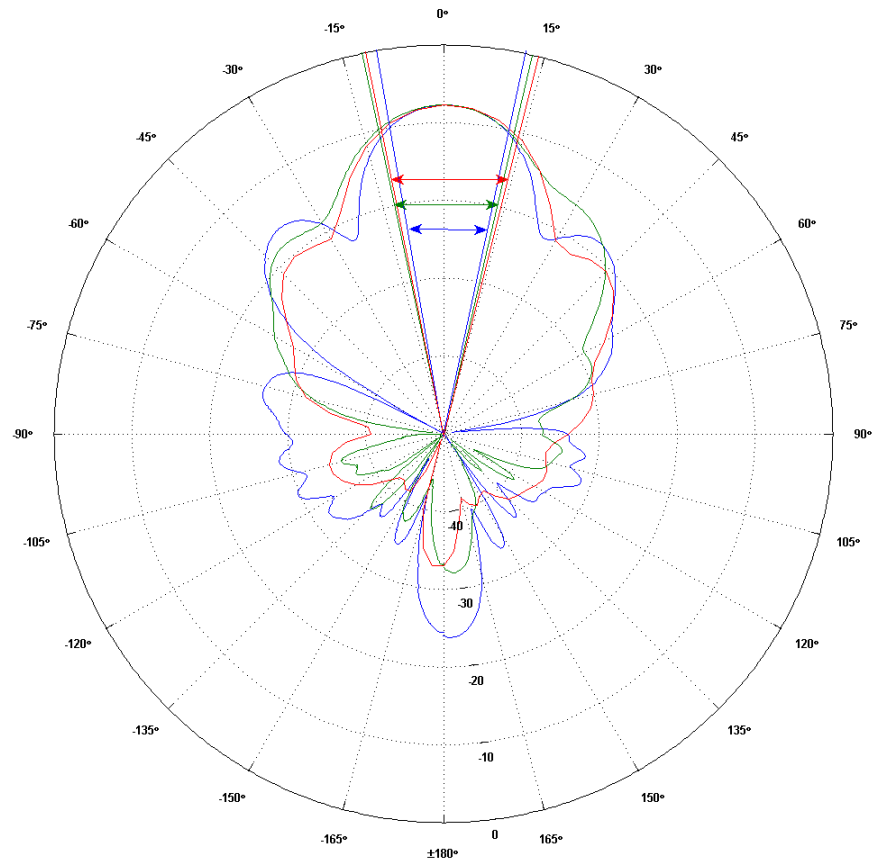


Figure D.11: The field pattern with half power beam width for the helical antenna measured for 2.185 GHz. The blue and green plots are for the transmitting horn antenna in horizontal and vertical position. The red plot is results from the simulation.

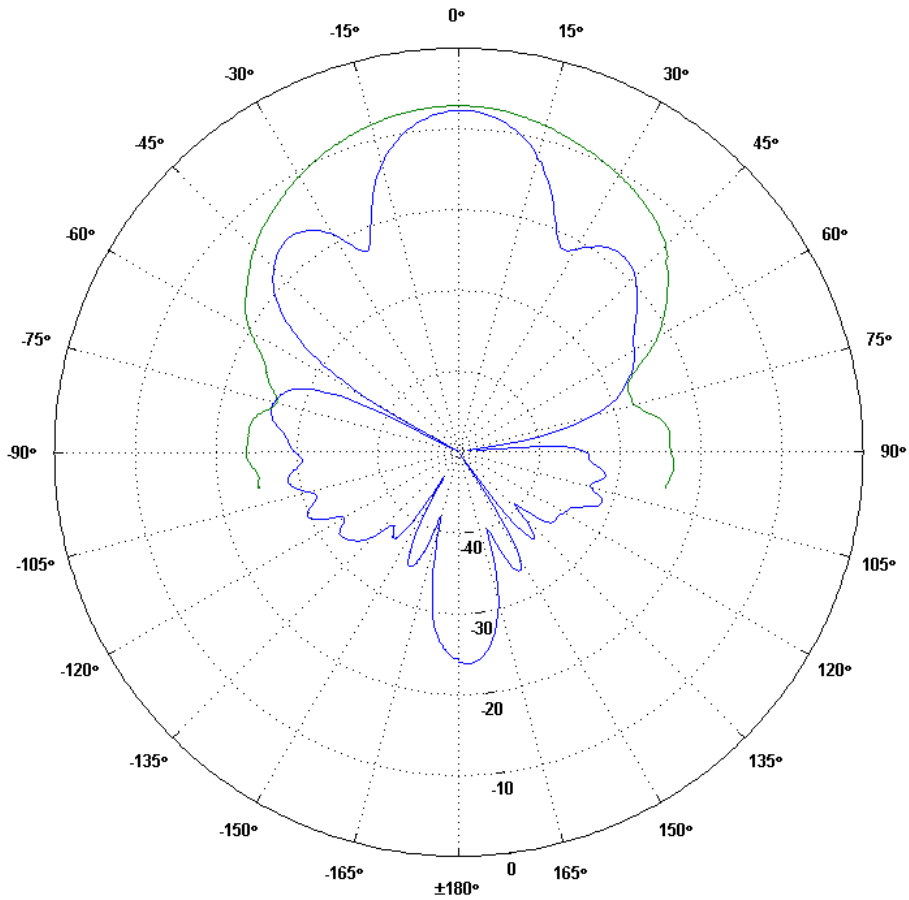


Figure D.12: The field pattern measured for the helical antenna marked blue compared with the field pattern for the reference horn antenna marked green.

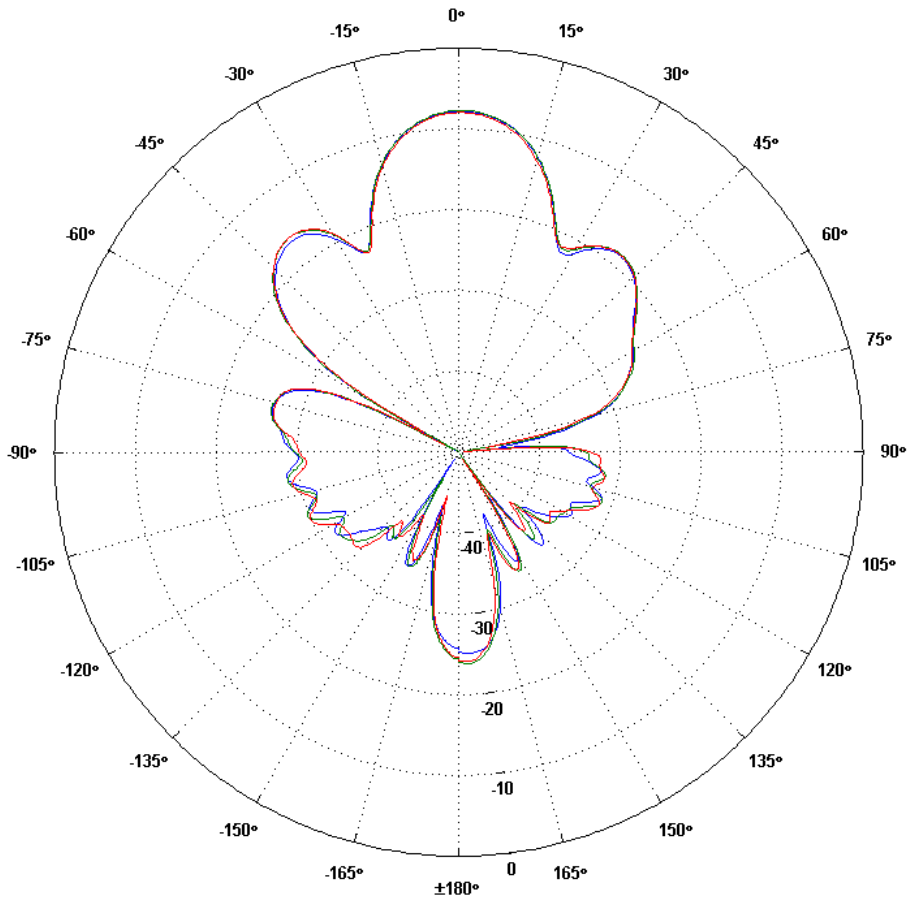


Figure D.13: Comparison of the field pattern for different frequencies. 2.175 GHz is marked blue, 2.185 GHz is marked green and 2.195 GHz is marked red. Measurements are done with horizontal polarization of the transmitting horn antenna.

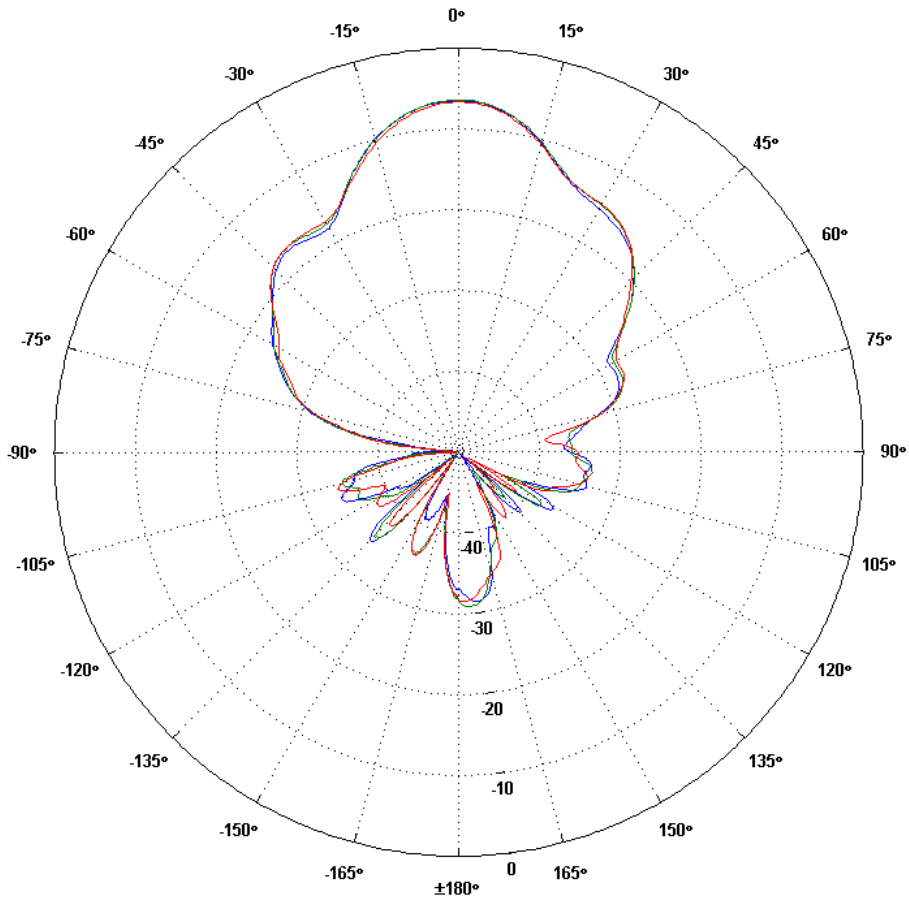


Figure D.14: Comparison of the field pattern for different frequencies. 2.175 GHz is marked blue, 2.185 GHz is marked green and 2.195 GHz is marked red. Measurements are done with vertical polarization of the transmitting horn antenna.

## D.4 Comparison between measurements with the three different ground conductors

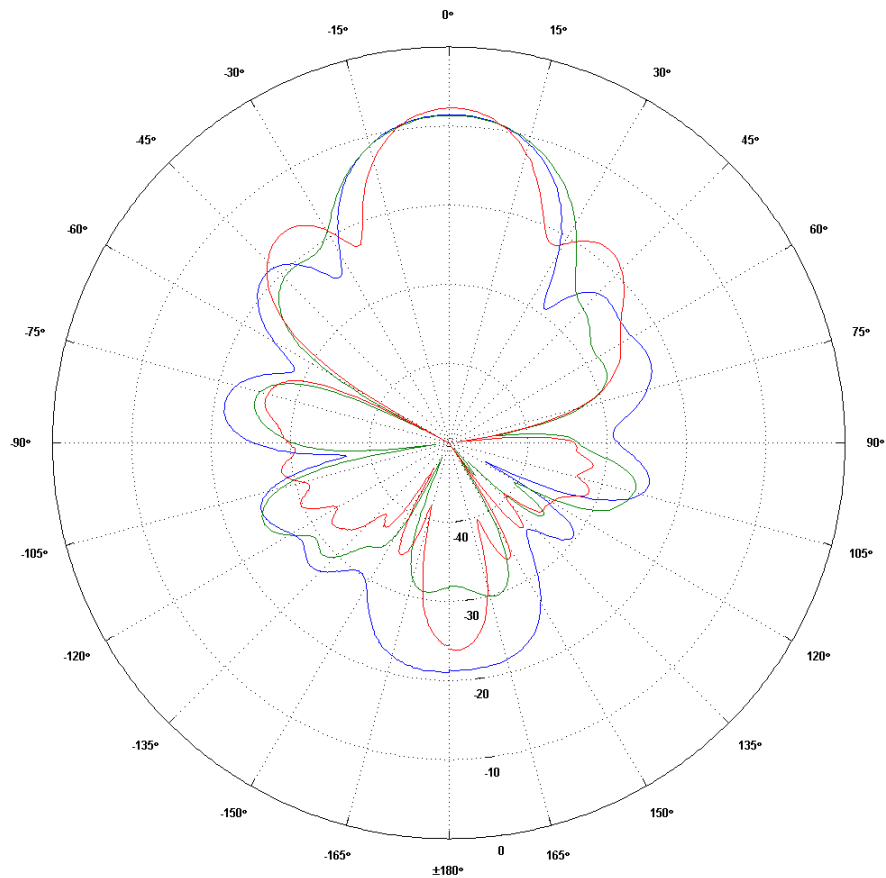


Figure D.15: The horizontal field pattern for the ground conductors. The flat ground conductor is marked blue, the cupped ground conductor is marked green and the truncated cone ground conductor is marked red.

## D.5 Impedance matching

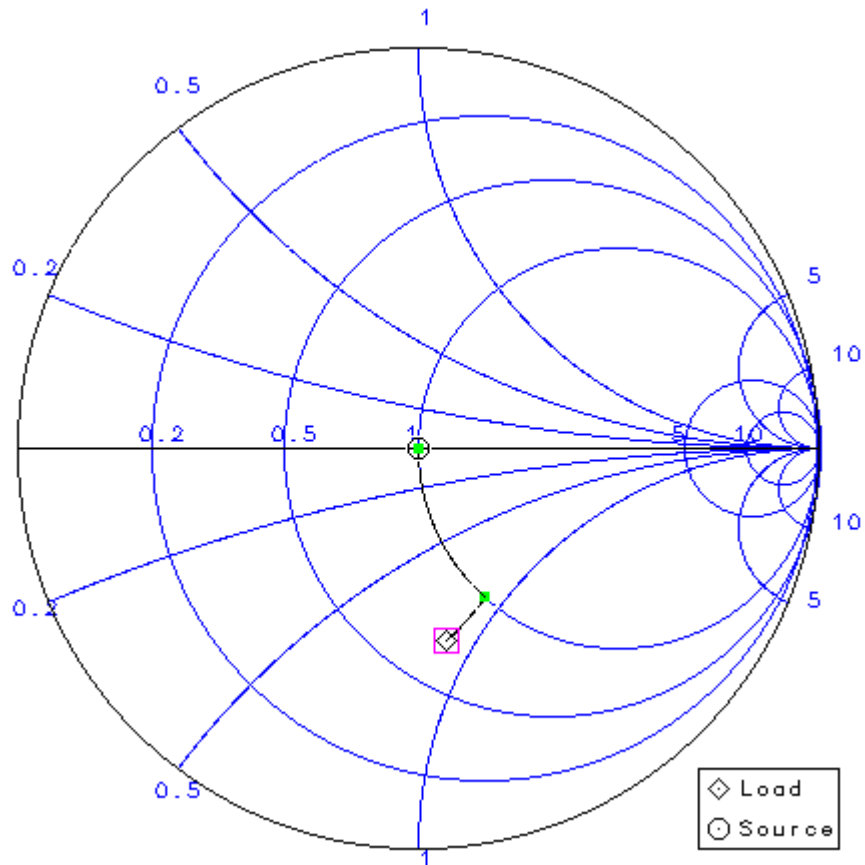


Figure D.16: The Smith chart shows the reflection at the input port for the helical antenna. Before impedance matching, the normalized reflection at the input port is  $S_{11} = 0.022 - j0.446$ .

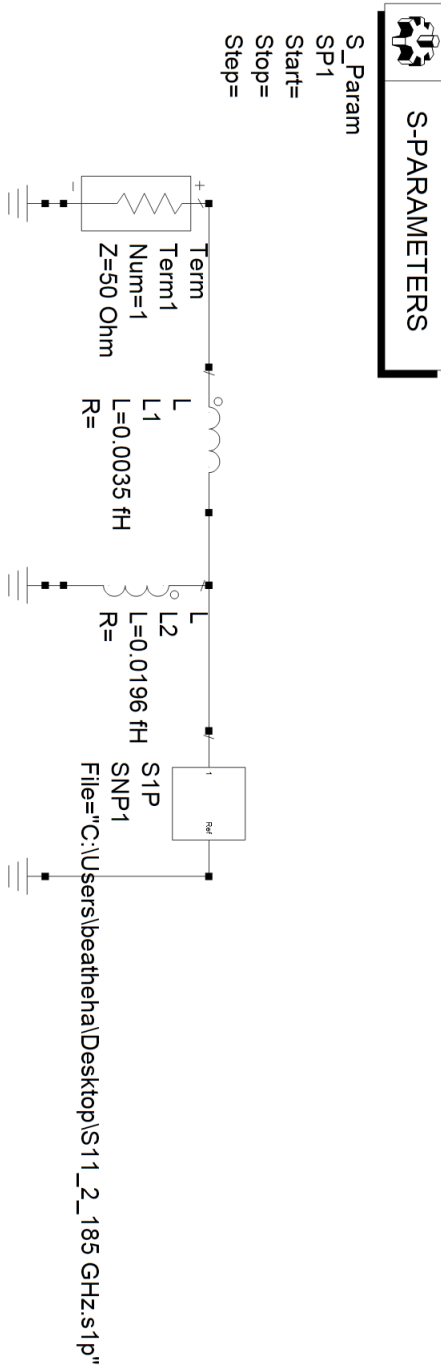


Figure D.17: Impedance matching circuit for the antenna, solved as an one port problem in ADS with 50  $\Omega$  termination.